Archaeological and Anthropological Sciences

# How much do we know about glassy materials in Bronze and Iron Ages Italy? New data and general overview.

--Manuscript Draft--

| | |
|---|---|
| **Manuscript Number:** | AASC-D-18-00007 |
| **Full Title:** | How much do we know about glassy materials in Bronze and Iron Ages Italy? New data and general overview. |
| **Article Type:** | Original Paper |
| **Section/Category:** | Glasses |
| **Corresponding Author:** | Sonia Conte, Ph.D.<br>Consiglio Nazionale delle Ricerche<br>ITALY |
| **Corresponding Author Secondary Information:** | |
| **Corresponding Author's Institution:** | Consiglio Nazionale delle Ricerche |
| **Corresponding Author's Secondary Institution:** | |
| **First Author:** | Sonia Conte, Ph.D. |
| **First Author Secondary Information:** | |
| **Order of Authors:** | Sonia Conte, Ph.D. |
| | Ilaria Matarese |
| | Giovanna Vezzalini |
| | Marco Pacciarelli |
| | Teodoro Scarano |
| | Alessandro Vanzetti |
| | Bernard Gratuze |
| | Rossella Arletti |
| **Order of Authors Secondary Information:** | |
| **Funding Information:** | |
| **Abstract:** | Knowledge about glass trading in protohistoric Southern Italy has been limited by the few archeometrical data available to date, which prevented a comparison between the well-known Northern trend. The aims of this work is, therefore, to fill the gap in data relative to the Bronze-Iron Ages Southern vitreous items, in order to make possible a general overview of the protohistoric Italian glassy supply routes. The paper presents physical-chemical data of sixty-one vitreous items coming from eleven Southern Italian sites, dated from the beginning of the Bronze Age up to the Archaic period (22th-6th century BC), ensuring a complete diachronic analysis. SEM-EDS, EMPA, LA-ICPMS and XRD analyses allowed the definition of raw materials and manufacturing techniques employed, and also the determination of the items provenance. The sample set shows a great variability of glass chemical types, being composed by plant ash glass, mixed alkali and natron samples. A complex picture, mostly related to the different natron glass typologies (High-Zr, Low-Zr, Black,…) and their fast technological evolution in the early 1st millennium BC, emerges. Taking into account the data reported in this study and those available in literature relative both to Northern and Southern Italian Bronze-Iron Ages items, this work demonstrates, for the first time, the existence of different trade routes. This is especially true for the early periods - Early/Middle Bronze Ages, whit Northern Italy involved in the trades with Central Europe, while South already inserted in the Mediterranean interactions. |

| | |
|---|---|
| **Suggested Reviewers:** | Julian Henderson<br>julian.henderson@nottingham.ac.uk |
| | Ian Freestone<br>i.freestone@ucl.ac.uk |
| | Natalie Venclova<br>venclova@arup.cas.cz |

# How much do we know about glassy materials in Bronze and Iron Ages Italy? New data and general overview.

Conte Sonia[1*], Matarese Ilaria[2], Vezzalini Giovanna[3], Pacciarelli Marco[2], Scarano Teodoro[4], Vanzetti Alessandro[5], Gratuze Bernard[6], Aletti Rossella[7]

[1] *CNR-ISTEC, via Granarolo 64, 48018 Faenza (RA), Italy.* *Corresponding author, e-mail:sonia.conte@istec.cnr.it. Telephone number: +390546699777

[2] *Department of Humanistic Studies, University of Naples Federico II, Corso Umberto I, 40, 80138 Naples, Italy*

[3] *Department of Chemical and Geological Sciences, University of Modena, via Campi 103, 41100 Modena, Italy*

[4] *Department of Cultural Heritage, University of Salento, Piazza Tancredi 7, 73100 Lecce, Italy*

[5] *Department of Antiquity, Sapienza University of Rome, Piazzale Aldo Moro 5, 00185 Rome, Italy*

[6] *Institut de Recherche sur les ArchéMATériaux, CNRS/Université d'Orléans, Orléans, France*

[7] *Department of Earth Sciences, University of Turin, Via Tommaso Valperga Caluso, 35, 10125 Turin, Italy*

## ABSTRACT

Knowledge about glass trading in protohistoric Southern Italy has been limited by the few archeometrical data available to date, which prevented a comparison between the well-known Northern trend. The aims of this work is, therefore, to fill the gap in data relative to the Bronze-Iron Ages Southern vitreous items, in order to make possible a general overview of the protohistoric Italian glassy supply routes. The paper presents physical-chemical data of sixty-one vitreous items coming from eleven Southern Italian sites, dated from the beginning of the Bronze Age up to the Archaic period (22$^{th}$-6$^{th}$ century BC), ensuring a complete diachronic analysis. SEM-EDS, EMPA, LA-ICPMS and XRD analyses allowed the definition of raw materials and manufacturing techniques employed, and also the determination of the items provenance. The sample set shows a great variability of glass chemical types, being composed by plant ash glass, mixed alkali and natron samples. A complex picture, mostly related to the different natron glass typologies (High-Zr, Low-Zr, Black,…) and their fast technological evolution in the early 1$^{st}$ millennium BC, emerges. Taking into account the data reported in this study and those available in literature relative both to Northern and Southern Italian Bronze-Iron Ages items, this work demonstrates, for the first time, the existence of different trade routes. This is especially true for the early periods – Early/Middle Bronze Ages, whit Northern Italy involved in the trades with Central Europe, while South already inserted in the Mediterranean interactions.

**KEYWORDS:** archaeometry; glass; Bronze and Iron Ages; Southern Italy; trace elements; provenance.

### Acknowledgements

The authors are indebted to Dr. Massimo Tonelli (Centro Interdipartimentale Grandi Strumenti-Unimore) for help with the (E)SEM analysis. The *Museo archeologico regionale eoliano "Luigi Bernabò Brea"* is acknowledged for providing the Lipari samples, while Dr. Pierfrancesco Talamo is acknowledged for providing the Pompei-Sant'Abbondio sample.

## 1. INTRODUCTION

In the last decades, the analytical study of the ancient glass allowed an extraordinary advance in understanding the ancient world (for a summary see Henderson 2013). The determination of the physical-chemical properties of glass artifacts is complementary to the traditional tools used for the archaeological investigations, and offers the chance to understand the materials employed for the glass production and the level of technology reached. It is worthnoting that this combined approach can sheds light not only on the ancient technologies but on the connection/exchange among different contexts of antiquity. This represents a powerfull tool especially concerning the pre/protohistoric period, when the lack of written sources make difficult unravel the trade routes.

To date, the research on the Italian protohistoric glass has been mostly focussed on the Bronze Age vitreous materials found in Northern Italy (e.g.: Angelini et al. 2002, 2004, 2005, 2006; Towle et al. 2001). These quite large amount of data allowed the identification of local specialised manifactures, like those of Frattesina dated to the Final Bronze Age (e.g.: Angelini et al. 2004). Somewhat has been done also for the Northern glass of the subsequent period, the Early Iron Age (Angelini et al. 2011; Polla et al. 2011; Arletti et al. 2011a; Conte et al. 2016b). Opposite to the relative well-known situation of the North, the vitreous materials found in the Southern contexts are almost unknown. Few data are available for the Bronze Age (Angelini et al. 2003; Conte et al. 2015), while the works of Conte and co-workers (2016a, b), shed the first light on the complex situation of the Early Iron Age, characterised by the co-existence of many different chemical types (HMG, LKHM and LMG glass). Despite the few data, a complex evolutionary picture of the glass technology at the transiton between the Bronze and the Iron Ages ($2^{nd}$-$1^{st}$ millennium BC) already emerges. From the technological point of view, in fact, this is a key period in the development of the glassmaking, with the demise of the plant ash technology in favour of the natron production. The glass produced at that moment represents therefore an important chronological and geographical link between the Late Bronze Age glassmaking technologies and the beginning of the long Greco-Roman tradition.

In this respect, to fill the data gap relative to the South and go deeper in this topic, data relative to 61 vitreous samples from eleven sites in Southern Italy covering a time span from the Early Bronze Age ($22^{th}$-$18^{th}$ centuries BC) to the end of the Archaic period ($6^{th}$ century BC), are reported. Specifically, the samples are coming from: Grotta Cardini (CZ – Late Eneolithic/Early Bronze Age, $22^{th}$-$18^{th}$ cent BC), Pompei (NA – Early Bronze Age, $18^{th}$-$17^{th}$ cent. BC), Vivara (NA – Middle Bronze Age 2, $16^{th}$-$15^{th}$ cent. BC), Murgia Timone (MT – Middle Bronze Age 3, $15^{th}$-$14^{th}$ cent BC), Broglio di Trebisacce (CZ – Final Bronze Age, $12^{th}$-$10^{th}$ cent BC), Lipari (CT – Final Bronze Age, $12^{th}$-$11^{th}$ cent BC), Roca Vecchia (LE – Final Bronze Age, $12^{th}$-$10^{th}$ cent BC), Torre Castelluccia (TA – Final Bronze Age, $12^{th}$-$10^{th}$ cent BC), Torre Galli (VV – Early Iron Age 1/Orientalising-Archaic period, $9^{th}$-$6^{th}$ cent BC), Francavilla Marittima (CZ – Early Iron Age 2/Orientalising period, $8^{th}$-$7^{th}$ cent BC), and Amendolara (CZ – Orientalising-Archaic period, $7^{th}$-$6^{th}$ cent BC).

Aims of this work are: *i)* to provide a complete physical – chemical characterization of the ancient glass finds by a multi-technique approach, defining the raw materials and the manufacturing techniques used for their production; *ii)* to suggest hypotheses regarding the provenance of protohistoric glass found in Southern Italy; *iii)* to compare the Northern and Southern Italian glass in order to highlight similarities or differences in the their supply routes. Therefore, this work will consider both the new data here reported and those available in literature, in order to offer, for the first time, a general review of our knowledge on this topic.

## 2. MATERIALS

The sampling strategy was aimed to the selection of glass from Southern Italy covering the entire period from the Early Bronze Age to the Archaic period, ensuring a complete diachronic analysis. The objects were selected following criteria of shape and colour, on both synchronic and diachronic base. Similar items – but related to different periods and/or sites – were included.

Table 1 reports the characteristics of all the analysed samples. Various glass chips were removed from beads with decorations in order to determine the composition of the bulk glass and that of the decorations. The sample list follows a chronological order. Regarding the relative chronologies reported in Table 1, the Bronze Age is subdivided into: Early Bronze Age-EBA ($22^{th}$-$18^{th}$ century BC), Middle Bronze Age 1-MBA1 ($17^{th}$-$16^{th}$ century BC), Middle Bronze Age 2-MBA2 (End $16^{th}$-$15^{th}$ century BC), Middle Bronze Age 3-MBA3 (End $15^{th}$-$14^{th}$ century BC), Recent Bronze Age-RBA ($13^{th}$-$12^{th}$ century BC) and Final Bronze Age-FBA (End $12^{th}$-$10^{th}$ century BC). The Early Iron Age 1 and 2 correspond

to the 9th and 8th century BC, respectively, while starting from the last quarter of the 8th to the 6th century BC the samples are attributed to the Orientalising/Archaic period. In the following a summary description of each site is given.

### 2.1. Grotta Cardini

Grotta Cardini is a cave located near Praia a Mare, close to Cosenza (Calabria). Luigi Bernabò Brea (Bernabò Brea et al. 1989) identified three archaeological deposits: lower layer (with pottery dated mainly to the Late Eneolithic and in part to the EBA), middle layer (MBA2) and upper layer (MBA3). The bead here analysed (sample GC2a) comes from the lower layer, in particular from the cutting III of the corridor (Bernabò Brea et al. 1989). It belongs to the flattened-globular type, a very popular type, diffused both in the Mediterranean and in the Aegean world during the Bronze Age and reprents the oldest glassy faience bead found in Southern Italy to date (up to now the oldest glassy bead in Central-Southern Italy was found at the *Villaggio delle Macine* on the Albano Lake, dated to the MBA 1-2 (Bellintani et al. 2007, fig. 1)).

### 2.2. Pompei-S. Abbondio

Pompei is located near Naples, in Campania. The site of Sant'Abbondio is a cemetery dated from the end of the EBA to the beginning of MBA (Mastroroberto and Talamo 2001; Mastroroberto 1998a, b). The sample here analysed (PM1g) (inv. 59530b) comes from the inhumation burial n. 26 of the necropolis, along with a bronze pin with discoidal head (Talamo, personal communication) dated to the EBA (Carancini 1975). The PM1g sample belongs to a segmented cylindrical faience bead, green in colour. It is the oldest faience bead attested in Southern Italy, while in the Center and in the North of Italy faience beads (with the same segmented cylindrical typology) were documented in contexts dated to the EBA-MBA1, as Lavagnone (Angelini et al. 2007, figure 1), Prato di Frabulino (Casi et al. 1995, figure 7:1), Grotta Regina Margherita (Angle et al. 2010, figures 3:4, 8:9).

### 2.3. Vivara

Vivara is a small island located in the Phlegraean Archipelago, very close to the island of Procida (Campania). High 120 m above sea level, Vivara overlooks the Ischia Channel and a large part of the Gulf of Naples. The high and steep slopes surrounding the island provided a natural defence against potential aggressors. During the first half of the second millennium BC, the special geographical and strategic location made it a formidable outpost in the Central-Southern Tyrrhenian area for the control of transmarine routes. Five beads were found at the site of Punta D'Alaca, dated to the MBA2. Four of the five beads were found in the so-called "fossa alpha", an hypogeic circular structure of probable ritual use. Below a burned organic layer, together with the beads, also some fragments of bronze brooche, shards of metal vessels, fragments of indigenous and Aegean imported pottery (dated to TE II) and a gold applique, were found. The type of items led to assume a ritual use of religious or funerary nature for this hypogeic structure (Giardino and Pepe 1998). There are three disc-shaped beads with rounded edge, one globular bead and one flattened-globular bead. These types of beads are very popular both in Italy and in the Aegean and Eastern world throughout the Bronze and the Iron Ages. Unfortunately, among the glass beads, only the globular one (sample V1l) shows a residue of un-weathered glass, which has been analysed, while the other ones are completely weathered.

### 2.4. Murgia Timone

Murgia Timone is located close to Matera on the Murge plateau, in the inner part of Basilicata Region. In this site some MBA chamber tombs accessed through a shaft were found. Tomb 1 of Murgia Timone was the subject of archaeological investigations in 1898 by Giovanni Patroni (Patroni 1898), which took most of the materials to the National Archaeological Museum of Naples. It is a chamber tomb found intact, with collective depositions: about 54 inhumations in the chamber and 22 in the shaft. In addition to the pottery equipment, dated to the MBA2-3 (Matarese 2016, cds), the tomb conserved a remarkable group of ornaments made up of bronze, bone, amber and glass. Among the ornamental items, there were seven glass beads, six of which (five flattened-globular, one globular) are coming from the chamber, one globular bead from the shaft. Unfortunately, only one flattened-globular bead (MT2t, belonging to the group found in the burial chamber) has preserved a portion of not altered glass that allowed the chemical analysis.

### 2.5. Broglio di Trebisacce

The site of Broglio is located close to the modern town of Trebisacce, near Cosenza (Calabria). It is one of a series of protohistoric settlements, occupying the first hills around the Sybaris coastal plain, whose northern edge is precisely at Trebisacce. The site, surrounded by steep slopes that offer a natural protection, is composed by a system of terraces at various levels, 2 km from the marine coastline. The highest of these terraces, the so-called "acropolis" (where the main excavation area is located) reaches the altitude of 180 m above sea level. Other terraces inside the geomorphological unit, such as the "Castello", closer to the plain and now heavily eroded, have preserved settlement layers. Starting from 1979 it was the subject of systematic excavation campaigns under the direction of R. Peroni and collaborators, and recently under that of A. Vanzetti (University La Sapienza of Rome).The remains of habitations and of productive, storage and defensive structures dating from MBA to EIA, have been brought to light (Peroni and Trucco 1994; Peroni and Vanzetti 2008). The bead here analysed, a barrel light-blue bead with white spiral decoration, was found in the FBA layers (BDT1l and BDT1w). It is a very common type in Frattesina productions from the 12$^{th}$ century BC.

**2.6. Lipari – Piazza Monfalcone**

Lipari is an island of the Aeolian archipelago, located in the Tyrrhenian Sea, in front of Northern coast of Sicily. A large necropolis belonging to the Ausonio II culture group and dated to the Final Bronze Age 1-2 was found at the Piazza Monfalcone site. One sample from the Tomb 18 (MON1b) and six samples from the Tomb 31 (MON2b, MON3g, MON4l, MON5l, MON6g and MON7l) were analysed in this study. Tomb 18 is a pithos burial closed by a slab. Among the funerary objects found inside there were a bronze fibula, a barrel shaped blue glass bead decorated with white spirals, a fragment of amber, nine green and eight blue glass beads (Bernabò Brea and Cavalier 1960). Based on the objects there found, it is very likely that it was a female burial. The richest tomb of the whole necropolis is the Tomb 31. It is a pithos characterised by the presence of a particularly high number of ornamental elements. Specifically, the grave goods include three rock-crystal beads, twenty-three amber beads, one necklace made up of 36 coloured glass and lithic beads and one necklace made up of 614 glass and faience beads. What is striking is not only the abundance of the material, but also the wide variety of bead types. The beads from which were taken the samples analysed belong to the discoidal type, widely attested in Italy and in the Aegean during the Bronze Age.

**2.7. Roca Vecchia**

The archaeological site of Roca is located on a calcareous promontory, near Lecce, on the Adriatic coast of Puglia. The protohistoric Roca site was occupied without interruption from the MBA2 (15$^{th}$ century BC) to the Final Bronze Age. This was probably due to the importance of its geographical position – at the narrowest passage of the Otranto Channel – and the richness in natural resources of its territory. The protohistoric settlement was protected by a large fortification wall running from North to South across the isthmus and marking the boundary of the inhabited area along the landward side (Scarano 2012). The site is characterised by an internal organization of the space of the settlement. The major evidences are related to the FBA. At this period belongs the so-called "great hut-temple", a monumental building destroyed by a massive fire. The quantity and quality of the materials found on the floor (ceramic, hard material animal, metal, etc.) are of exceptional importance, related to the daily activities and ceremonial practices (characterised by the presence of symbols of the Aegean world). Moreover, in a hole dug in the ground of the "great hut -temple", known as the "Ripostiglio degli Ori", were found two gold foils ("solar discs"), objects related to ornaments (fibulae, necklaces, bracelets, pendants, buttons, etc…), weapons and tools (daggers, spearheads, knives, axes, chisels, a drill, punches, awls, a hammer, a saw), ingots and scraps, bronze, shell, ivory and glass objects (Maggiulli 2009; Scarano and Maggiulli 2014). The samples here analysed (RC2b1, RC2b2, RC2b3, RC3b1, RC3b2, RC4t, RC6g, RC7g, RC8b, RC11b, RC12b, RC13b, RC14t, RC14w, RC15t, RC15w, RC16l, RC17t, RC18t, RC20g) come from this "Ripostiglio degli Ori", and belong to discoidal, eyes beads, and flattened globular types.

**2.8. Torre Castelluccia**

At the coastal site of Torre Castelluccia, located about 17 kms South-East of Taranto, an important fortified settlement flourished since MBA. The glasses here analysed were sampled from two discoidal beads belonging to a polimateric necklace, made up of glass, carnelian and bone beads. This necklace comes from the so-called "lumber-room" of the rectangular hut no. 7. This structure (where also amber beads were found) was built and used during the Final Bronze Age (Gorgoglione et al. 1993).

**2.9. Torre Galli**

Torre Galli is located on the Tyrrhenian side of Calabria. The site is known for the necropolis excavated by Paolo Orsi in the 1922-23, who discovered 334 graves, a large majority of which are single inhumation burials, characterised by the presence of rich, both male and female, grave goods. Among these, 280 tombs belong to the initial phase of the Early Iron Age (9th century BC, samples TG1l, TG5l, TG7inc, TG8l, TG9l, TG10l, TG11bl, TG14l ,TG17l), the others to the Archaic period (7th and especially 6th century BC, samples TG3bl, TG12bl, TG12w, TG13bl, TG13w). The items taken into account in this study are discoidal, barrel, cylindrical, globular, flattened-globular, polylobated and eyes beads. The protohistoric funerary goods belong to a thriving indigenous community, with a complex socio-economic and political-military organization, that entertained very early exchange relations with Levantine navigators (Pacciarelli 1999), while the late graves pertain to a final phase of the same indigenous center, that had close relations with the Greek subcolony of Hipponion.

### 2.10. Francavilla Marittima

The protohistoric settlement and cemetery of Francavilla Marittima are located close to the inner edge of the Sybaris coastal Plain, in Calabria. The samples here examined come from the Macchiabate necropolis. They are all related to the second phase of the Early Iron Age (FM2y, FM3inc, FM4inc, FM5a, FM6l, FM7bl, FM8bl, FM8y, FM9y, FM11a), dating to the 8th century BC, with the exception of the archaic sample FM10a (flattened globular bead), dating to the 7th century BC. The samples belong to discoidal, globular or flattened globular beads, with the exception of FM8bl-y which belongs to a ribbed cylindrical bead with a spiral decoration. Moreover, pear and flower pendants, and a spindle whorl, are present. The tombs at Macchiabate are clustered and overlapping, thus generating mounds, extending over rather large areas: the most completely explored case is that of Temparella (from which sample FM2y comes). The depositions of the 7th and 6th century BC are placed in close connection with the former Early Iron Age tombs, occupying the free spaces among them or with a direct overlap (Ferranti and Quondam 2006; Luppino et al. 2010).

### 2.11. Amendolara

The MBA-EIA settlement of Amendolara (Ionian Calabria, Southern Italy) occupied the plateau on which the medieval and modern town is located. After the Greek foundation of Sybaris, a new indigenous settlement rose a kilometer northern, on the San Nicola terrace. Probably this settlement belongs to the archaic necropolis of Paladino Ovest, excavated by J. De La Genière (2012). The burials, dating mainly to the 7th and 6th century BC, are arranged in regularly aligned groups, with nuclei of inhumed adult tombs separated by rows of infant ones, often buried into pithoi or other types of vessels (e.g. graves 73-76). The sample here examined (AM1g), which belongs to a biconical bead, comes from the grave 60/60bis at Paladino Ovest (Luppino et al. 2010).

## 3. EXPERIMENTAL METHODS

This study was carried out with a multi-technique and micro-distructive approach. The analyses were carried out by Scanning Electron Microscopy (SEM), Electron Microprobe (EMPA) for all the samples. Laser Ablation Inductively Coupled Plasma Mass Spectrometry (LA-ICPMS) analyses were performed on the transparent samples, while X Ray Diffraction (XRD) on the opaque ones. The good state of preservation of the glass allowed the removal of only small chips of few hundreds $\mu m^3$. For the EMPA analyses, the fragments sampled from the glass artefacts were mounted in an epoxy resin and polished using a series of diamond paste from 6 to 1µ. To prevent charging a carbon coating was applied to the polished sections. The same samples were used for SEM investigations.

### 3.1. Scanning Electron Microscope (SEM)

For this study backscattered electron images (BSE) and energy-dispersive spectra (EDS) were collected using a ESEM Quanta 200 environmental electron scanning microscope, equipped with an energy dispersive spectrometer SATW at the Centro Interdipartimentale Grandi Strumenti of the University of Modena and Reggio Emilia. The analyses were performed applying an acceleration voltage of 20 kV and a working distance of 11 mm. EDS spectra were analysed by the software INCA. The analyses were performed on the same polished and carbon coated samples subsequently used for the EMPA. BSE images were collected on all the glass samples to check the matrix homogeneity and EDS analyses were run to obtain qualitative and semiquantitative chemical analyses of the inclusions.

### 3.2. Electron Microprobe analysis (EMPA)

The chemical analyses of 17 major and minor elements were carried out using a Cameca SX 50 microprobe equipped with four scanning wavelength-dispersive spectrometers (WDS). The reference Smithsonian glass A standard (Jarosewich 2002) was employed as primary reference sample. Details of analytical conditions, applied standards, and accuracy and precision of the measurements are reported in supplementary material S1 and S2 of Conte et al. 2016a, being the samples analysed in the same run. Since the BSE images and EDS analyses evidenced the presence of many inclusions (particularly in the mixed alkali and black samples, see paragraph 4.3), ten points were analysed to test homogeneity and the mean value was calculated (standard deviation below 0.5). The only exclusion is represented by the opaque sample BDT1w, which is highly weathered, and only one point analysis gave good results. The EMPA results are reported in Table 2. The elements Ti, Co, Cu, Sn, and Sb were also measured with LA-ICPMS.

### 3.3. Laser-ablation inductively coupled plasma mass spectrometry (LA-ICPMS)

For this study LA-ICPMS was used to determine the concentration of 33 trace elements. The trace elements analysis was performed on all the transparent glasses, with the exclusion of samples TC1l, TC3l and TG11bl, due to their small size. The opaque samples were not analysed due to their heterogeneity. The analyses of the samples were carried out at the IRAMAT Centre Ernest-Babelon (CNRS/Univ. Orleans, France). The ablation system consists of a NeodymeYAG laser working at 266 nm (quadrupled frequency) coupled with a Thermo Electron Finnigan ELEMENT XR mass spectrometer (full details in Gratuze 2013). Standard Reference Material NIST612 (Pearce et al. 1997) was used as a reference sample to check precision and accuracy (its analysis is reported in supplementary material S3b of Conte et al. 2016a). As regards the samples, the standard deviations among the analysed points were below 10% for all the elements, with the exclusion of Cr, with more variable and high SD. In Table 3 and in the entire study, only Cr data with SD $\leq$10% were reported and considered. The results of the 50 transparent glass investigated are reported in Table 3 for the trace elements and 4 for the Rare Earth Elements (REE).

### 3.4. X Ray Diffraction (XRD)

X-ray diffraction experiments were performed on the opaque samples to identify crystalline phases dispersed in the glass matrix. Due to the small quantity of material available, the samples were mounted on a goniometric head and the experiments were carried out with a four-circle single crystal diffractometer Bruker X8-Apex with MoKα radiation, equipped with an area detector. The diffraction patterns were collected with a detector-sample distance of 40 mm and a time exposure variable between 60 and 120 s, depending on the amount of crystalline phases present in the glass. The diffraction rings were integrated using the Fit2d software programme (from 5 to 30° 2θ) and the patterns were then interpreted using the PDF database (McLune 1989).

## 4. RESULTS

### 4.1. Major, minor and trace elements composition

The chemical analyses of the major elements show a wide range of compositions. Silica contents range from 48.5% to 78.4%, soda from 1% to 21%, potash from 0.06% to 18.6%, lime from 0.9% to 10.5%, magnesia from 0.3% to 7% and alumina from 0.1% to 5.6% (Table 2):

FIGURE 1

The traditional comparative analysis of the $K_2O$-MgO contents (Fig. 1), indicators of the fluxing agent used (e.g. Sayre and Smith 1961; Henderson 1988a, 1989), allows to distinguish three maxi-groups:

1) Low MgO-High $K_2O$ glass, consisting of thirty samples. Based on the potash and soda levels, this group can be divided into two sub-groups: *i)* HIGH-K glass represented by four samples (three from Roca Vecchia-RC6g, RC7g and RC14w- and one from Torre Castelluccia-TC3l) with very high potash (13.4-18.6%) and low soda (1-5%), and *ii)* MIXED ALKALI glass composed by twenty-six samples (two from Broglio di Trebisacce-BDT1l and BDT1w, five from Lipari-Piazza Monfalcone -MON1b, MON2b, MON4l, MON5l and MON7l, seventeen from Roca Vecchia - RC2b1, RC2b2, RC2b3, RC3b1, RC3b2, RC4t, RC8b, RC11b, RC12b, RC13b, RC14t, RC15t, RC15w, RC16l, RC17t, RC18t and RC20g, one from Torre Castelluccia-TC1l, and 1 from Torre Galli-TG1l), characterised by comparable levels of potash and soda (7.6-9.8% $K_2O$, 5.7-8.3% $Na_2O$) (Table 2). All the HIGH-K and MIXED ALKALI samples are characterised by very low levels of lime (2% CaO, on average).

2) High MgO glass (3-7% MgO and 1.3-3.6% $K_2O$). These fourteen samples (one from Pompei-PM1g, one from Vivara-V1l, one from Murgia Timone-MT2t, two from Lipari-Piazza Monfalcone-MON3g, MON6g, two from Francavilla Marittima-FM3inc, FM6g, seven from Torre Galli-TG5l, TG7inc, TG8l, TG9l, TG10l, TG14l, TG17l) are also characterised by high soda (18%) and high lime (6.5%), as recorded for glass produced with plant ash as fluxing agent (e.g: Henderson 2013).

3) Low MgO-Low $K_2O$ glass (0.3-1.5% and 0.1-1.4%, respectively). This group is composed by seventeen samples (one from Grotta Cardini-GC2a, nine from Francavilla Marittima-FM2y, FM4inc, FM5a, FM7bl, FM8bl, FM8y, FM9y, FM10a, FM11a, six from Torre Galli-TG3bl, TG11bl, TG12bl, TG12w, TG13bl, TG13w, one from Amendolara-AM1g), which always show MgO and $K_2O$ values $\leq$1.50%, typical of glasses made with natron as flux (e.g: Henderson 2013). From the chemical data of major elements it is possible to recognise some peculiar chemical features among this natron glass: *i)* the yellow opaque glass (all from Francavilla Marittima-FM2y, FM8y, FM9y) show very high PbO and $Sb_2O_5$ levels (~30% and ~3.3%, respectively); *ii)* the white opaque glass (from Torre Galli-TG13w) show high $Sb_2O_5$ (~7%); *iii)* the black glass (from Francavilla Marittima-FM7bl, FM8bl, and Torre Galli-TG3bl, TG11bl, TG12bl, TG13bl) show very high FeO contents (3.8-14.6%). The other samples, instead, show the classic characteristics of the natron transparent glass, and will be therefore named "classic natron".

Despite the HIGH-K and MIXED ALKALI samples show different alkalis contents, they are characterised by the same trace elements pattern (Fig. 2), with the highest Rb (120 ppm) and the lowest Sr concentrations (113 ppm) of the whole sample set. The concentrations of the other trace elements, as well, is very similar in two sample sets showing a rather depleted pattern (Fig. 3). Likewise, the samples of the PLANT ASH group show a very homogeneous composition (Tables 3-4), exhibiting a depleted pattern of almost all the elements, with the exclusion of Sr, present in the highest concentration of the sets (Figure 2). NATRON samples exhibit a more complex composition. Based on the major and minor chemical compositions, the natron glasses have been already subdivided into: *classic* natron, opaque yellow and white, and black specimens. Considering that trace elements analyses were not performed on the opaque samples, the remaining *classic* natron and black glasses show distinctive fingerprints. Among the *classic* natron it is possible to distinguish: *i)* Natron Low-Zr glass (FM5a, FM10a, FM11a), showing the lowest trace (excluding Sr and Ba) and REEs concentrations of the set (Fig. 2 and 3), and *ii)* Natron High-Zr samples (AM1g and FM4inc) characterised by the highest Zr and Hf levels of the set, and by trace and REEs contents higher than those observed for the Natron Low-Zr and PLANT ASH glasses (Fig. 2 and 3).

FIGURE 2

The composition of the BLACK glasses (both for major/minor and for trace elements) is rather variable. Specifically, the black samples TG3bl, TG12bl and TG13bl, from Torre Galli, show the same trace and REEs trend of the Natron High-Zr glass, while those from Francavilla Marittima (FM7bl, FM8bl) are very different, with the highest levels of Ti, V, Cr, Ga, Y, Th and all the REEs of the whole set.

FIGURE 3

Finally, the sample GC2a shows a distincitive trace elements pattern being characterised by high Ga, Sr and Ba, associated to a REEs pattern less depleted (Figure 3).

### 4.2. Colourants

The samples show a wide range of colours: three are colourless, four amber, six black, three opaque yellow, five opaque white, seven green, eleven blue, twenty-two light blue/turquoise. The composition of colourless samples (Plant Ash: FM3inc and TG7inc and Natron: FM4inc) excludes the use of any decolouring agent. The final effect is due to the use of pure raw materials, suitable for the production of high quality colourless glass, as confirmed by the chemical data (Table 2). Similarly, the natron amber samples FM5a, FM10a, FM11a exhibit low levels of alumina (0.2% on average), indicating the use of pure vitrifying raw materials. The amber shade originates form the low levels of iron combined to the furnace conditions, which can impart different nuances to the final glass, also when iron is present in small amount (Gliozzo 2017). On the contrary, the amber sample GC2a shows a higher iron content (0.5% FeO), responsable for its nuance.

The green Plant Ash-MON3g and Natron-AM1g samples owe their pale colour to the presence of iron (Table 2), as well. The remaining five green samples (Plant Ash-PM1g, MON6g, High-K-RC6g, RC7g, and Mixed Alkali-RC20g) are strongly coloured by the copper contents (2.1% $Cu_2O$ on average).

The light blue/turquoise samples (Plant ash-V1l, MT2t, FM6l, TG5l, TG8l, TG9l, TG10l, TG14l, TG17l, Mixed Alkali-BDT1l, MON4l, MON5l, MON7l, RC4t, RC14t, RC15t, RC16l, RC17t, RC18t, TC1l, TG1l, and High-K- TC3l) are coloured by the addition of copper (0.9% and 5.1% $Cu_2O$, on average respectively). The natron black specimens (FM7bl, FM8bl, TG3bl, TG11bl, TG12bl, TG13bl) due their colour to the presence of iron (3.7-14.6% FeO).

Blue samples (MON1b, MON2b, RC2b1, RC2b2, RC2b3, RC3b1, RC3b2, RC8b, RC11b, RC12b, RC13b) are all Mixed Alkali glass. They are coloured by variable amounts of copper (0.3-2% $Cu_2O$), high cobalt levels (0.08-0.12% CoO) and show high nickel (2500 ppm on average) and arsenic (1470 ppm) levels, positively correlated.

The origin of the opacity will be discussed in the section 4.4. From the chemical point of view, it is worth noting the presence of high levels of antimony in white samples, and of coupled antimony and lead in the yellow ones. TG12w and RC15w (white decoration of black and blue turquoise samples, respectively) show high level of iron (5% FeO) and copper (2.1% $Cu_2O$) deriving from coloured glass bodies on which they lyes.

### 4.3. ESEM-EDS data

The BSE images revealed the presence of various inclusions, mostly in the mixed alkali and in the natron black samples. All the other transparent samples appear homogeneous, and dispersed particles are absent.

The BSE image of sample RC2b3 (Figure 4) well summarises the features observed in mixed alkali samples. They are characterised by the presence of many primary air bubbles and dispersed residual quartz grain. When cracks are present, the rims show lower contrast, justified by the lack of sodium and potassium. This alkali leaching is a typical feature of glass which undergone weathering.

FIGURE 4

The BSE images of the Francavilla natron black samples show a poor melting quality (Figure 5). The glass is characterised by the presence of numerous unmelted crystals (probably feldspar grains), high atomic number inclusions (probably iron oxides) and primary air bubbles.

FIGURE 5

In contrast, the BSE images of the Torre Galli natron black glass TG13bl revealed homogeneous glass matrix with little primary gas bubbles and only few grains of residual quartz (Fig. 6).

FIGURE 6

### 4.4. XRD data

The X-ray diffraction experiments were carried out on the white and yellow opaque glass present as decorations on the beads body (BDT1w, RC14w, RC15w, FM8y, FM9y, TG12w, TG13w), and on the yellow monochromatic opaque bead FM2y. The patterns of BDT1w, RC14w and TG12w did not show diffraction peaks, suggesting that the number of particles dispersed in the samples is too low to be detected, while for the other samples the analyses proved the presence of crystalline phases. Specifically, the white opaque sample TG13w contains calcium antimonate in its hexagonal phase $CaSb_2O_6$, while white glass RC15w owes its opacity to the presence of quartz. The diffraction patterns of the yellow samples (FM2y, FM8y and FM9y) clearly show the presence of a lead pyroantimonate with $Pb_2Sb_2O_7$ stoichiometry. These are very well-known opacifiers, employed almost from the beginning of glass production (1500 BC) up to the Roman period (Turner and Rooksby 1959; Tite et al. 2007) to produce white and yellow opaque glass.

## 5. DISCUSSION

### 5.1. Major, minor and trace elements compositions

#### *5.1.1. PLANT ASH glass*

Fourteen samples from Pompei, Vivara, Murgia Timone, Lipari-Piazza Monfalcone, Francavilla Marittima and Torre Galli, have been classified as PLANT ASH glass, on the basis of the potash and magnesia levels. This was the first glass production technology employed from the 2nd millennium BC until the 10th-9th cent BC, based on the use of ashes from halophytic plants and silica (Turner 1956; Forbes 1957; Henderson 1985; Henderson 2000). The resulting glass, showing high levels of magnesia (c. 2-6%) and potash (c. 0.5-4% $K_2O$), and then called High Magnesium Glass (HMG) (Sayre and Smith 1961), was widespread among the strongly hierarchical Late Bronze Age societies in Mesopotamia, Egypt, and Greece (*e.g.* Nolte 1968; Barag 1970; Henderson 2013) and was present in some Western Mediterranean sites dating from the Bronze Age through to the Early Iron Age (*e.g.* Hartmann et al. 1997; Santopadre and Verità 2000; Angelini et al. 2002; Gratuze and Billaud 2003; Nikita and Henderson 2006; Conte et al. 2016a). In this respect, recent data relative to Late Bronze Age glass found in Romania, Germany and Denmark (Varberg et al. 2015, 2016), further confirmed the incredible spread of the HMG glass during this period.

The PLANT ASH samples of this study are all dated between the 18th and the 8th century BC. Their general chemical signature exhibits a low impurity pattern (e.g. low alumina, low titania). Alumina could derive from the ashes and/or from the processing of plants, e.g. residual clay. Moreover, in a recent experimental work Rehren (2016) demonstrated that even if pure quartz (such as quartz pebbles with no impurities) was used for the HMG glassmaking, the introduction of other elements into the glass batch could derive from the quartz grinding. The transformation of the coarse quartz pebbles into very fine powder silica, in fact, is a necessary step for glass melting. Depending on the mineralogical composition of the rock used for the grinding tools, elements such as Al, Fe, Ti, K, Ca, can contaminate the final glass. Likewise, the Cr can derive from the stones used as tools in the crushing and grinding of the quartz pebbles (Rehren 2016).

The use of a very clean silica source, is confirmed by the strongly depleted REEs pattern and by the low concentration of Nd (2.2 ppm). Nd in glass is in fact introduced with the mineral fraction present in silica sand (clay and mainly heavy minerals) (Degryse and Shortland 2009). On the other hand, the PLANT ASH samples show the highest levels of strontium of the set, associated with high lime contents (Tables 2 and 3). Ca and Sr in plant-ash glass derive from the ashes of halophytic plants used as flux, in which calcium is a major common constituent, producing glass with CaO levels typically ≥5% (Wedepohl et al. 2011a). The CaO/Sr ratio of the plant-ash glass here studied (186) is not far from that found by Freestone et al. (2003) for plant ash glass from Banias-Israel (CaO/Sr ratio 220), and by Conte et al. (2016a) for plant ash glass from Sarno e Capua (213).

#### *5.1.2. MIXED-ALKALI and HIGH-K glass*

The twenty-six MIXED ALKALI (LMHK) samples (from Broglio di Trebisacce, Lipari-Piazza Monfalcone, Roca Vecchia, Torre Castelluccia and Torre Galli) show a texture characterised by the presence of many primary air bubbles and relict grains of residual quartz, typical of this glass type (Henderson 1988a, b; Santopadre and Verità 2000; Towle et al. 2001). MIXED ALKALI glass is a chemical type widely spread in the Final Bronze Age Europe (12th-10th century BC). It has been recognised by several authors in glass from France (Guilaine et al. 1990; Gratuze et al. 1998; Croutsch et al. 2011), Switzerland (Henderson 1993), Germany (Hartmann et al. 1997), Bohemia – Czech Republic (Venclovà et al. 2011), England and Ireland (Henderson 1988a, b), and Greece (Henderson 1993; Nikita and Henderson 2006). This glass is completely different from the predominant coeval glass type-HMG, and does not have a chemical counterpart outside Europe. For these reasons, it is considered a typical European production. Specifically, the Final Bronze Age site of Frattesina (Veneto-Italy) is a key site, which has produced the largest amount of LMHK raw glass and artefact to date (Brill 1992; Towle et al. 2001; Angelini et al. 2004).

In our sample set a small group of four samples (from Roca Vecchia and Torre Castelluccia), labelled HIGH-K, is characterised by very high potash levels, lower soda levels and higher lime contents when compared to the LMHK.

The HIGH-K composition is less diffused, and represented by only few specimens found in Northern Italy (Towle et al. 2001; Angelini et al. 2004), Bohemia (Venclovà et al. 2011) and France (Gratuze 2013). This particular composition represents a potash pole of the LMHK glass. As observed by Gratuze (2013), while the classical LMHK glass is quite resistant to corrosion, its potash rich counterpart seems to strongly suffer from weathering effects. The fragility of these beads – often nearly entirely corroded – may explain why they are less represented in a large part of the studied Bronze Age sites.

The MIXED ALKALI and HIGH-K samples of this study are all dated between the 12th and the 10th century BC (with the exclusion of sample TG1l dated to the 9th cent BC), perfectly fitting the Final Bronze Age production period. Almost all of them are blue and light blue/turquoise in colour. As already observed by Brill (1992) for LMHK glass from Frattesina, the light blue/turquoise glass were coloured with copper only, while the blue samples contain copper in variable amounts, as well as cobalt. The cobalt is accompanied by high levels of nickel and arsenic, positively correlated, suggesting the use of the mineral skutterudite [(Co,Fe,Ni)$As_3$] as cobalt source. This mineral, in fact, has been found in the German Black Forest (HahnWeinheimer 1995), and, according to many authors (e.g. Towle et al. 2001), it could had been used as cobalt source for the production of blue glass in the European Final Bronze Age. The plot of FeO *vs*. CuO (Figure 7) reports the literature values of Cu-blue/turquoise and Co-blue LMHK glasses from Italy (Frattesina/Maricorda -Towle et al. 2001; Frattesina/Poviglio -Santopadre and Verità 2000) and Greece (Nikita and Henderson 2006), compared to those of our samples, confirming their similarity.

FIGURE 7

The general chemical signature of the MIXED ALKALI and HIGH-K glass shows a pattern characterized by rather low impurity levels (Figures 2 and 3), with the exclusion of Rb. Rb, together with Ba, is usually interpreted as indicator of K-feldspar, micas and clay minerals presence in the sand. In this case, the levels of alumina (1.8% on average, with the exclusion of sample RC14w with 5.6% $Al_2O_3$), and in general the depleted REEs pattern, allow to exclude this hypothesis. Rb and Ba, due to their geochemical affinity with K, are highly present in glass made with ashes of continental plants (Wood Ash Glass, Wedepohl et al. 2011a). It can be therefore assumed that Rb in the LMHK glass here analysed mostly derived from the plant ashes used as flux as also suggested by Shortland and Schroeder (2009) and confirmed by Barkoudah and Henderson (2006). If purified plant/wood ashes were used as a source of alkali then the relatively low strontium (113 ppm on average) associated with low calcium (2% CaO) would be expected, since the calcium levels would have been reduced by the ash purification (Venclovà et al. 2011).

### *5.1.3. NATRON glass*

Seventeen samples (from Grotta Cardini, Torre Galli, Francavilla Marittima and Amendolara) are characterised by low contents of $K_2O$ and MgO, both <1.5%, and classified as natron glass. It is assumed that this glass type was made using as flux mineral soda, which in antiquity was mostly extracted in Egypt (Turner 1956; Henderson 2000; Shortland et al. 2006; Purowski et al. 2012). From the early first millennium BC, the use of natron spread through the Mediterranean and Levantine regions. Around the 10th century BC, in Egypt, some glassmakers started to use this mineral (natron) as an alkali source (Schlick-Nolte and Werthmann 2003) producing the so called low magnesium glass (LMG). To date, literature records only few cases that evidence the use of natron in the early 1st millennium BC, with examples coming from Nimdur (Reade et al. 2005), Hasanlu (Brill 1999), Sarno and Capua (Conte et al. 2016a), and Bologna (Polla et al. 2011; Conte et al. 2016b).

The natron glass samples of this study are all dated to the Iron Age – Orientalising/Archaic period, with the exclusion of sample GC2a from Grotta Cardini, which is dated to the Eneolithic/Early Bronze Age, appearing too ancient for this kind of flux. The low magnesium low potassium composition (labelled LMLK by Angelini et al. 2005) recorded for this sample (whose flux source is still uncertain – Tite et al. 2008) has been also found in some later glassy faience beads, from Italy (Conte et al. 2015; Santopadre and Verità 2000; Angelini et al. 2005) and Mycenaean Greece (Tite et al. 2005), dated to the Middle and Recent Bronze Age. To date, GC2a is the most ancient LMLK sample ever found and could be compatible with local small scale production. The chemistry of these LMLK glassy faience beads is quite variable indicating the use of different sources for both vitrifying and colorant agent. The trace elements analysis of the sample GC2a, with high levels of Ga and Ba in association to high amount of alumina, confirms the use of an impure sand.

The other sixteen samples of the Natron group, dated between the 9th and the 6th century BC, can be subdivided in: *i)* classic natron; *ii)* opaque yellow and white samples; *iii)* black glass.

*5.1.3.1 Classic natron*

They can be further divided in low-Zr and high-Zr.

The low-Zr glass shows a high purity composition with the lowest value of alumina, magnesia, potash, iron and REE of all the sample set. These chemical characteristics are consistent with the use of quartz pebbles. The use of a Ca-free

vitrifing agent required the deliberate addition of lime. The relatively low Sr content associated with a rather high Ca/SrO ratio (362), could be an indication of the addition of diagenetically altered shells partially recrystallized after the loss of their initial strontium contents (Wedepohl et al. 2011a). In fact, Sr in natron glass is mostly derived from shells (when Ca/SrO ratio is <200) or limestone (Ca/SrO >600) (Wedepohl and Baumann 2000; Freestone et al. 2003; Brems et al. 2013).

The high-Zr glass shows high and strongly correlated amounts of Zr and Hf, indicating that they were introduced with zircon ($ZrSiO_4$), the most abundant heavy mineral in quartz sand (Götze and Lewis 1994; Degryse and Shortland 2009; Wedepohl et al. 2011a, b; Brems and Degryse 2013). Moreover, the high level of Y can be related to the presence of garnet (Wedepohl *et al.,* 2011a), while the REEs are less depleted with respect to the low-Zr glass. Anyway, their general low content and the rather flat distribution pattern testify the high maturity of the sand used (Götze and Lewis 1994), rich in quartz and zircon and relatively depleted in other heavy minerals (McLennan 1989; Freestone et al. 2000, 2002; Brems and Degryse 2013). The glass stabilizer used is probably the same used for the low Zr glass being the Sr content and Ca/SrO ratio very similar.

*5.1.3.2 Opaque samples*

These samples show the same characteristics of classic natron samples and, in addition, show high levels of lead and antimony, due to the lead and calcium antimoniates used as opacifying, as enhanced by the XRD analyses.

*5.1.3.3 Black samples*

Studies on Iron Age ($10^{th}$-$8^{th}$ century BC) black glass carried out by Gratuze and Picon on French samples (2006), Reade and co-workers on Jordanian glass (2009), and Conte and co-workers on Italian and Slovakian glass (2016a, b) demonstrated that natron black glass are among the first natron glasses ever produced. All the samples analysed from Italy, France and Jordan show the same chemical features, characterised by low potash and magnesia, very high iron, low lime along with high levels of trace and rare earth elements. Consistently, (E)SEM-EDS analyses – when performed – evidenced the presence of many unmelted grains of heavy minerals (*e.g.* chromite, iron oxides) (Reade et al. 2009; Conte et al. 2016a, b).

It is possible to hypothesise that the first recipe to produce natron glass followed the two-ingredients' tradition adopted for centuries in the plant ash technology: vitrifying plus flux. In the case of the black glass: highly impure sands (probably dark in colour and purposely selected) mixed directly with natron. The glassmakers who first passed from ashes (containing rather high levels of Ca) to natron (Ca free) did not recognise the role of the lime as stabiliser and granter of glass durability. These natron black glass of the early $1^{st}$ millennium BC survived to the weathering thanks to iron, acting as "alternative stabiliser" – in the same way in which natron early Al-Co blue glass survived thanks to the presence of Al (for a detailed discussion see Conte et al. 2016a). Most the other early natron glass produced in this period is likely to have been lost (Shortland et al. 2006).

The oldest black samples here analysed (TG11bl, FM7bl and FM8bl, $9^{th}$-$8^{th}$ century BC) fit in the frame of earliest natron glass produced above summarised. They show low lime, high iron and high trace elements and REE contents (i.e. Ti, V, Cr related to the presence of iron oxides and cromites, Y related to garnet and Th to both zircon and monazite (Gromet & Silver 1983; McKay 1989; McLennan 1989)). The presence of residual unmelted grains (i.e. feldspars and iron-oxides) further confirms the use of impure sands.

On the other hand, the more recent samples (TG3bl, TG12bl and TG13bl, $7^{th}$-$6^{th}$ century BC) are characterised by lower alumina, titania, and iron and higher lime with respect to the older ones. Trace and REEs patterns indicate the use of mineralogically mature sand, rich in quartz and zircon and depleted in heavy minerals, which is the same sand used for the production of Natron High-Zr descrived above (Fig. 2-3, paragraph *5.1.3.1*). The backscattered electron images confim this assumption, showing an homogeneous matrix, characterised by the presence of few unmelted quartz grains.

These samples are the first evidence of the technology refinement in the production of the natron glass during the $1^{st}$ millennium BC with the choice of lime-rich sands (or the separate addition of lime to the glass batch) to improve the glass durability. The new recipe – based on the use of natron and mineralogically mature sands, with lime contents high enough to stabilise the glass – allowed obtaining a high quality glass, which could successively be coloured in different nuances. This is evident if we consider that the more recent natron black glasses were made with the same sands of green and colourless samples (Natron High-Zr glass). It worth be noticed that this was the technology employed during

the subsequent Roman period, when black glass was made starting from typical natron-based glass, to which iron was added in the forms of iron ores (Group IIB, Van der Linden et al. 2009), hammer scale (Rehren et al. 2012; Cholakova and Rehren 2012), or pure magnetite (Group BG3, Cagno et al. 2014).

**5.2. Trace elements signature: comparison with literature data.**

A detailed comparison between trace element composition of the present samples and the coeval glass productions was conducted in order to hypothesise the provenance of the glass items.

The sample GC2a from Grotta Cardini – although not very precisely dated, since the layer of provenance yielded finds chronologically spanning from 2800/2700 to 2000/1900 BC – is likely the oldest of the whole sample set and shows a LMLK composition (found in some Middle and Recent Bronze Age glassy faience). The trace elements signature of this sample is compared with the data available in literature for glass with: *i)* a LMLK composition sample, PZ FP3 found at Punta di Zambrone (13$^{th}$ century BC) (Conte et al. 2015); *ii)* the prehistoric predominant chemical type: Mesopotamian and Egyptian HMG (Shortland et al. 2007). Figure 8 clearly documents the distinct composition of sample GC2a with respect to the other. At this stage of knowledge, a possible local small scale production can be suggested.

FIGURE 8.

The trace element composition of the Plant ash glass of this study (18$^{th}$-8$^{th}$ century BC) has strong similarities with those of samples found in Sarno and Capua (8$^{th}$-7$^{th}$ century BC, Conte et al. 2016a) and Mesopotamian glass (Shortland et al. 2007), opposite to the Egyptian samples (Shortland et al. 2007) (Fig. 9).

FIGURE 9

It has been demonstrated that the main discriminatory elements which allow to distinguish between the Mesopotamian and Egyptian Plant Ash glass production are lower Ti, Zr, La and higher Cr for the Mesopotamian one (e.g. Walton et al. 2009; Jackson and Nicholson 2010; Varberg et al. 2015, 2016). The cause of these differences was attributed in the different petrologic nature of the grinding tools employed for powdering quartz pebbles: basic rocks in Mesopotamia (such as ophiolites, basalt and amphibolites) acidic rocks (diorite – granite series) in Egypt (Rehren 2016).

In this respect, the comparison of chromium/lanthanum and zirconium/titanium ratios (Figure 10) of the Plant ash glass here analysed with those produced in Egypt and Mesopotamia (Shortland et al. 2007), clearly shows that our samples from Southern Italy are compatible with a Mesopotamian origin.

FIGURE 10

The Mixed alkali and High-K samples of this study (12$^{th}$-9$^{th}$ century BC) were compared to coeval LMHK glass found in France (Croutsch et al. 2011) and Bohemia (Venclovà et al. 2011) and supposed (on the basis of formal-typological and chemical characteristics) to be imported from Frattesina, the only one production site attested for this period, to date. Figure 11 evidences the strong similarity of all these samples, enriched in Rb and depleted in the other trace elements.

FIGURE 11

The first isotopic investigation on LMHK glass found in Frattesina (Henderson et al. 2015), revealed the presence of two different isotopic signatures: one compatible with raw materials located near Frattesina, and the other compatible with a more southern silica source (sands near Rome). It is interesting to observe that the chemical fingerprint with a Central Italy compatibility has been found in a glass with a HIGH-K chemistry. Anyway, this isotopic study is preliminary and many other specific analyses will be necessary to investigate the possible presence of any other FBA LMHK production site. At this stage of knowledge, it is likely to assume that the LMHK (mixed alkali and HIGH-K) from Roca Vecchia, Broglio di Trebisacce, Lipari and Torre Galli here analysed, were probably imported from the Northern Italian site of Frattesina.

The Natron low-Zr and high-Zr samples (including the natron black from Torre Galli) of this study (8$^{th}$-6$^{th}$ century BC) were compared with coeval natron glass found in Italy (Sarno and Capua -Conte et al. 2016a), and later specimens from a Georgian site dated to the 5$^{th}$ century BC (Shortland and Schroeder 2009), Roman sites dated to the 1$^{st}$–3$^{rd}$ century AD

(Degryse and Shortland 2009), and Central Iraqi sites dated to the 1st–5th century AD (Mirti et al. 2008) (Figure 12). The comparison highlights that the only glass produced with quartz pebbles is the Natron low-Zr samples (8th-7th cent. BC) here analysed. On the contrary, high-Zr samples and the black glass from Torre Galli show the same trace elements pattern of the Italian Iron Age/Archaic glasses (7th-6th cent. BC). Natron glass produced later (5th cent. BC-5th cent. AD) is very different, showing homogeneous patterns characterised by higher V, Sr, Y, and Ba, but lower Zr and Hf compared to the earlier productions. These data indicate that at the beginning of the natron production quartz pebbles were employed as silica source (low-Zr glass), then substituted by very mature quartz sands (7th-6th cent. BC high-Zr and black Torre Galli). Finally, starting from the 5th century BC less pure sands were used for the glass production and this new successfully and standardized recipe was used for ten centuries (5th cent. BC- 5th cent. AD).

FIGURE 12

The trace elements composition of the black glass from Francavilla Marittima (8th century BC) are compared in Figure 13 with that of coeval black glass coming from Sarno, Cuma, Pozzuoli and Bologna for which an Egyptian origin was hypothesised (Conte et al. 2016a, b). The pattern show similar trends. The variability in concentrations is the result of the use of very impure sands, coupled with the employ of not well-fixed recipes for the glass production. It is possible to hypothesise an Egyptian origin for Francavilla samples, as well.

FIGURE 13

### 5.3. Chemistry of the Italian protohistoric vitreous materials: a comparison between the North and the South of the country

Based on the available literature data and the results here discussed, a detailed comparison between the protohistoric vitreous materials from Northern and Southern Italy, is now possible. Unfortunately, the only work relative to the Nuragic culture of Sardinia (Angelini et al. 2012) does not report numerical data, preventing a precise comparison. Tables 5 and 6 show a summary of the results reached through this work.

#### *5.3.1. Early Bronze Age faience (22th-17th century BC)*

Sample GC2a is likely to be the most ancient Italian vitreous material studied to date, and also the most ancient vitreous material with a LMLK composition (never attested before the MBA3-RBA) and probably is related to small scale local production (see paragraph 5.3.3). Sample PM1g (Pompei-late EBA), shows a "Mesopotamia – like HMG" composition. This result is in contrast with the data relative to EBA Northern Italy (Lavagnone site, Angelini et al. 2006), where faience samples show a LMHK composition, typical of the European productions (also found in Slovakia (Angelini et al. 2006), Switzerland (Henderson 1993), and France (Gratuze et al. 1998)). These data suggest that while in the EBA the North of Italy was involved in the trade with the Central Europe, Southern Italy was already inserted in the Mediterranean interactions.

#### *5.3.2. Middle Bronze Age 1-2 glass (17th-15th century BC)*

Sample V1l, coming from Vivara (Naples) and dating to the MBA2, is a "Mesopotamia – like HMG", according to what found in samples from Grotta Manaccora (Apulia) (Angelini et al. 2003). On the contrary, in Central and Northern Italy, only LMHK glassy faience were found (Angelini et al. 2005). The pattern of circulation of vitreous materials is therefore consistent with that of EBA.

#### *5.3.3. Middle Bronze Age 3 and Recent Bronze Age glassy faience and glass (15th-12th century BC)*

The sample from Murgia Timone-Matera (MT2t), dated to the MBA3, is a "Mesopotamian – like HMG" glass. As far as the RBA is concerned, the glassy faience PZ FP3 (Punta di Zambrone-VV, Conte et al. 2015) shows a composition (LMLK) very similar to that found in other coeval glassy faience found in Northern Italy (Reggio Emilia and Poviglio, in Santopadre and Verità 2000), in Southern Italy (Trinitapoli and Cisternino, in Angelini et al. 2005), and also in Greece (Platanos and Psaro, in Tite et al. 2005). In the MBA3-RBA the same chemical types – HMG and LMLK – were found both in Northern and Southern Italy, with the exclusion of the HMBG (high magnesium brown glass), which probably is a Northern production (Angelini et al. 2005), not (yet) recorded in the South. The circulation of HMG glass and LMLK glassy faience in Italy in this period is probably related to the contacts with the Mycenaean palatial society.

#### *5.3.4. Final Bronze Age glass (12th-10th century BC)*

Four different FBA sites of Southern Italy were considered in this work: Broglio di Trebisacce-Cosenza (2 samples), Lipari Piazza Monfalcone (7 samples), Roca Vecchia-Lecce (20 samples) and Torre Castelluccia-Taranto (2 samples). Almost all the samples are LMHK/HIGK-K glass (probably) imported from Frattesina, with the exclusion of samples MON3g and MON6g, both from Lipari, which show a "Mesopotamiam – like HMG" composition. This is the first evidence of the LMHK glass presence in Southern Italy. The attestations of LMHK glass to date, in fact, were mainly relative to Northern Italy and Central Europe, with few cases in Greece. Nevertheless, while in Northen regions the massive presence of LMHK glass totally replaced the previously diffused HMG, the HMG glass from Lipari testifies the continuity in trade with the Aegeum/Near East.

#### *5.3.5. Early Iron Age 1-2 glass (9th-8th century BC)*

The glass items dating to the Early Iron Age 1-2 here analysed (9 from Torre Galli and 10 from Francavilla Marittima) are characterised by a wide range of chemical compositions, as expected for that period. The transition between the 2nd and 1st millennium BC, in fact, is one of the key periods in the development of glassmaking, with the replacement of the previous plant-ash technology with a natron-based production. Considering the samples from Torre Galli and Francavilla Marittima here studied, along with coeval glass coming from Sarno, Cuma and Capua (published in Conte et al. 2016a) five different chemical groups can be identified: *i)* Mixed alkali glass (1 sample from Torre Galli), imported from Frattesina; *ii)* Plant ash glass imported from Mesopotamia; *iii)* Natron glass with a likely Egyptian origin; *iv)* Natron Black glass rich in FeO (around 10%) with an Egyptian origin; *v)* Natron Al-Co blue glass – coloured with Egyptian cobaltiferous alum (see Conte et al. 2016a) – imported from Egypt.

These data testify both the appearance of new chemical types (new natron technology) and the continuity of Bronze Age traditions (e.g: the two ingredients' recipe of the natron black glass and the use of Egyptian cobaltifeous alum for the natron Al-Co blue glass). The same situation is found in Northern Italy. This is especially true for the Villanovan materials from Bologna contexts – pertaining to mixed alkali, classic natron, alumina-cobalt natron glass (Arletti et al. 2011a; Polla et al. 2011) and black natron samples (Conte et al. 2016b) – and for the Etruscan glass – pertaining to plant ash and natron composition (Towle and Henderson 2004). On the contrary, in the Golasecca area (Novara, Varese and Como provinces-Northern Italy) in the 9th century BC only mixed alkali glass were found (Angelini et al. 2011).

Finally, it is worth noting that the diffusion of natron glass – as demonstrated by the sample from Torre Galli – started earlier in Southern Italy (9th century BC), with respect to the North (8th century BC).

#### *5.3.6. Orientalising/Archaic glass (last quarter 8th-6th century BC)*

Considering the samples belonging to the Orientalising/Archaic period here analysed (1 from Francavilla Marittima, 5 from Torre Galli and 1 from Amendolara), along with data of coeval Sarno glasses (Conte et al. 2016a), four main different chemical groups were identified. Specifically: *i)* Natron black glass rich in FeO probably imported from Egypt; *ii)* Classic natron glass with a probable Egyptian origin; *iii)* Plant ash glass imported from Mesopotamia; *iv)* High-Al glass (with ~4% FeO and ~10% $Al_2O_3$ – see Conte et al. 2016a), probably produced with natron as flux.

These data evidence that some elements of the Bronze Age tradition still survive, as the ongoing use of plant ash glass, until the 7th century BC. The High-alumina group, dated to the last quarter of the 8th century BC, represents an uncommon chemical type with no comparison among the Italian ones, probably still belonging to a first natron production characterised by unusual compositions. On the contrary, the black and the classical natron samples (7th-6th century BC) testify the fast evolution of the natron glass, showing a higher chemical homogeneity if compared to those of the Early Iron Age 1-2.

The available literature data for Northern Italy are few. A sample set relative to 7th-6th century BC glass, belonging to the Golasecca culture (Angelini et al. 2011), shows a LMG composition, which is natron glass. Other literature data pertain to a later period, as Etruscan natron glass from Spina and Bologna dated to the 6th-3rd (Arletti et al. 2009, 2011b) and from Adria dated to the 5th-2nd century BC (Panighello et al. 2012), confirm the standardisation of the natron glass in that period. The very few data for 8th-6th century BC Northern Italian glass, do not allow a real comparison with our results. However, it can be definitely observed a progressive evolution and standardisation of the natron glass production, which reached its peak in Roman times.

## 6. CONCLUSIONS

The sixty-one Bronze and Iron Ages glasses from eleven different archaeological sites of Southern Italy, cover a chronological span beginning at least with the Early Bronze Age ($22^{th}$-$18^{th}$ century BC) and ending with the Archaic period ($6^{th}$ century BC), ensuring a complete diachronic analysis.

The results provided evidence of a great complexity in the chemical composition, production technologies and provenance of the glass items. In particular, this work clearly shows the complexity of the natron based glass category and provided evidence of the technology refinement in the production of the natron glass during the early $1^{st}$ millennium BC. Of particular interest, the black glasses produced with two different silica sources and recipes: the oldest samples ($9^{th}$-$8^{th}$ cent. BC) produced with very impure-iron rich sands directly mixed with natron, the more recent ones ($7^{th}$-$6^{th}$ cent. BC) with the same mature sand used for high quality natron-based glass and coloured by the addition of iron oxides.

A very interesting aspect of this work is that, for the first time, a detailed comparison between the protohistoric vitreous materials found in Northern and Southern Italy has been realised, demonstrating the existence of different trends. In the EBA and MBA1-2 the North of Italy was involved in the trade with Central Europe, while Southern Italy was already inserted in the Mediterranean interactions importing vitreous materials from Mesopotamia. In the MBA3-RBA the same chemical types were found both in Northern and Southern Italy, suggesting the circulation of exotic vitreous materials through all the country, as a consequence of the spread of the dominant Mycenaean trade network in the Central Mediterranean. The massive glass production at Frattesina during the FBA totally replaced the Near East materials in Northern Italy, in connection with the crisis of the Aegean world. Anyway, in Southern Italy both a continuity in trade with the Eastern Mediterranean – bringing Mesopotamian products – and the presence of Frattesina glass, are attested. This is the first evidence of Mixed Alkali glass presence in Southern Italy to date. The significance of the Cypriot/Near Eastern trade with Southern Italy, Frattesina and Sardinia in this period has to be reminded, too. In the EIA 1-2 a substantial dependence on Mediterranean trades, firstly established with Southern Italy (in the $9^{th}$ century BC), and then expanded to the North ($8^{th}$ century BC), is testified by the appearance of materials with a strong Eastern affinity (natron glass), in accordance with the spread of the Phoenician and Greek (Euboean, Corinthian, etc.) trade. Even if for the Orientalising/Archaic period the few data available for the Northern Italy do not allow a real comparison, it can be generally observed a progressive standardisation of the glassmaking processes and a continuity in the trade with the Eastern regions.

**REFERENCES**


Angelini I, Artioli G, Bellintani P, Diella V, Gemmi M, Polla A, Rossi A (2004). Chemical analyses of Bronze Age glasses from Frattesina di Rovigo. Northen Italy. Journal of archaeological Science, 31. DOI: 10.1016/j.jas.2004.02.015

Angelini I, Artioli G, Bellintani P, Diella V, Polla A, Recchia G, Residori G (2003). Materiali vetrosi da Grotta Manaccora e Coppa Nevigata: inquadramento archeologico e archeometrico nell' ambito della civiltà del bronzo italiana da il vetro in Italia meridionale e insulare. In: Piccioli C, Sogliani F. (eds) Atti del secondo congresso multidisciplinare.

Angelini I, Artioli G, Bellintani P, Diella V, Polla A, Residori G (2002). Project Glass materials in the Protohistory of North Italy, a first summary. In: d'Amico C (ed) Atti del secondo congresso nazionale di Archeometria. Patron Editore, Bologna, Italy, 581-595.

Angelini I, Artioli G, Bellintani P, Polla A (2005). Protohistoric vitreous materials of Italy: from Early faience to Final Bronze Age glasses. In Annales du 16e Congrès de l'Association Internationale pour l'Histoire du verre, Nottingham, UK 32-36.

Angelini I, Artioli G, Polla A, de Marinis R (2006). Early Bronze Age faience from north Italy and Slovakia: a comparative archaeometric study. In: Proceeding of the 34th symposium of Archeaometry, Zaragoza Spain, 371-378.

Angelini I, Nicola C, Artioli G (2012). Materiali vetrosi protostorici della Sardegna: indagini archeometriche e confronto analitico con reperti coevi. In: Proc. XLIV Riunione Scientifica dell'Istituto Italiano di Preistoria e Protostoria "La preistoria e la protostoria della Sardegna". Cagliari, Barumini, Sassari, 23-28 novembre 2009, IIPP, Firenze, pp. 1131-1150.

Angelini I, Nicola C, Artioli G, DeMarinis R, Rapi M, Uboldi M (2011). Chemical, mineralogical and textural characterisation of Early Iron Age vitreous materials from the Golasecca Culture (Northern Italy). In: Turbanti-Memmi I (ed) Proceedings of the 37th International Symposium on Archaeometry, Heidelberg, 26–32.

Angelini I, Polla A, Artioli G (2007). Archaeometric investigations of the ornamental faience beads from Lavagnone (BS). In: "Notizie Archeologiche Bergomensi", Museo Archeologico di Bergamo, 10, pp. 285-299.

Angle M, Catracchia F, Cavazzuti C, Celletti P, Malorgio M, Mancini D (2010). La grotta Regina Margherita a Collepardo (Frosinone). In: Ghini G (ed.) Atti del Convegno Sesto Incontro di Studi sul Lazio e la Sabina, Roma, 4-6.

Arletti R, Bertoni E, Vezzalini G, Mengoli D (2011°). Glass beads from Villanovan excavation in Bologna (Italy): an archaeometrical investigation. European Journal of Mineralogy, 23, 959968. DOI: 10.1127/0935-1221/2011/0023-2166

Arletti R, Maiorano C, Ferrari D, Vezzalini G, Quartieri S (2009). The first archaeometric data on polychrome Iron Age glass from sites located in Northern Italy. Journal of Archaeological Science, 37, 4, 703–712. DOI: 10.1016/j.jas.2009.11.001

Arletti R, Rivi L, Ferrari D, Vezzalini G (2011b). The Mediterranean Group II: analyses of vessels from Etruscan contexts in Northern Italy. Journal of Archaeological Science 38. https://doi.org/10.1016/j.jas.2010.10.028

Barag D (1970). Mesopotamian core-formed glass vessels (1500-500 B.C.). In: Oppenheim et al, 131-199.

Barkoudah Y and Henderson J (2006). Plant ashes from Syria and the manufacture of ancient glass: ethnographic and scientific aspects. Journal of Glass Studies, 48, 297–321.

Bellintani P, Angelini I, Artioli G, Polla A (2007). Villaggio delle Macine: le più antiche perle in vetro e ambra dell'Italia centrale. In: Atti della XL Riunione Scientifica dell'Istituto Italiano di Preistoria e Protostoria, Strategie di insediamenti tra Lazio e Campania in età preistorica e protostorica, Roma-Napoli-Pompei, 891-895.

Bernabò Brea L and Cavalier M (1960). La stazione preistorica della contrada Diana e la necropoli protostorica di Lipari. Meligunis Lipàra I, Palermo.

Bernabò Brea L, Biddittu I, Cassoli P F, Cavalier M, Scali S, Tagliacozzo A, Vagnetti L (1989). La Grotta Cardini (Praia a Mare- Cosenza): giacimento del Bronzo. In: "Memorie dell'Istituto Italiano di Paleontologia umana", n.s. 4, Roma.

Brems D, Degryse P (2013). Trace element analysis in provenancing Roman glass-making. Archaeometry, 56, 116–136. DOI: 10.1111/arcm.12063

Brems D, Ganio M, Latruwe K, Balcaen L, Carremans M, Gimeno D, Silvestri A, Vanhaecke F, Muchez P and Degryse P (2013). Isotopes on the beach, Part 1: strontium isotope ratios as a provenance indicator for lime raw materials used in Roman glass-making. Archaeometry 55, 2, 214–234.

Brill R.H. (1992). Chemical analyses of some glasses from Frattesina. Journal of glass studies 34, pp.11-22.

Brill R. H. (1999). Chemical analyses of early glasses: Volume 1 (tables) and Volume 2 (catalogue). Corning Museum of Glass, Corning, NY.

Cagno S, Cosyns P, Izmer A, Vanhaecke F, Nysc K, Janssens K (2014). Deeply colored and black-appearing Roman glass: a continued research. Journal of Archaeological Science 42, 128-139.

Carancini G L (1975). Die Nadeln in Italien. Gli spilloni nell'Italia continentale. Prähistorische Bronzefunde 13, Munchen.

Casi C, D'Ercole V, Negroni Catacchio N, Trucco F (1995). Prato di Frabulino (Farnese VT). Tomba a camera dell'età del Bronzo. In: "Preistoria e Protostoria in Etruria", Secondo Incontro di Studi "Tipologia delle necropoli e rituali di deposizione", 81-110.

Cholakova A and Rehren T (2012). Producing black glass during the Roman period-notes on a crucible fragment from Serdica, Bulgaria. In: Proceedings of 39th International Symposium for Archaeometry, Leuven, 261-267.

Conte, S., Arletti. R., Henderson, J., Degryse, P., Blomme, A. (2016b). Different glassmaking technologies in the production of Iron Age black glass from Italy and Slovakia. Archaeological and Anthropological Sciences. DOI 10.1007/s12520-016-0366-4

Conte S, Arletti R, Mermati F, Gratuze B (2016a). Unravelling the Iron Age glass trade in Southern Italy: the first trace element analyses. European Journal of Mineralogy, 28, 2, 409-433. DOI: 10.1127/ejm/2016/0028-2516

Conte S, Matarese I, Quartieri S, Arletti R, Jung R, Pacciarelli M, Gratuze B (2015). Bronze Age Vitreous Materials from Punta Di Zambrone (Southern Italy). European Journal of Mineralogy, 27, 337–351. DOI: 10.1127/ejm/2015/0027-2450

Croutsch C, Tegel W, Nicolas T, Pascutto É, Billot M, Leprovost C, Gratuze B, Logel T, Putelat O (2011). Les sites protohistoriques d'Erstein «Grasweg-Pae» (Alsace, Bas-Rhin): l'occupation Rhin-Suisse-France-Orientale. Revue Archéologique de l'Est, t. 60.

De la Genière J (2012). Amendolara: La nécropole de Paladino ouest avec une contribution de Fulvio De Salvia ; et une note de Stéphane Verger. Naples: Centre Jean Bérard.

Degryse P and Shortland A (2009). Trace elements in provenancing raw materials for Roman glass production. Geologica Belgica, 12, 135–43. DOI: 10.1111/arcm.12063

Ferranti F and Quondam F (2006). La prima età del ferro in Sibaritide: una rassegna delle sepolture. In: "Studi di Protostoria in Onore di Renato Peroni", pp. 590-601.

Forbes R.J (1957). Glass, in Studies in Ancient Technology, vol5, Leiden, pp. 110-231.

Freestone I C, Gorin-Rosen Y and Hughes M.J (2000). Primary glass from Israel and the production of glass in the late antiquity and the early Islamic period. In: M.-D. Nenna (Ed.), La route du verre: ateliers primaires et secondaires de verriers du second millénaire avant J.C. au Moyen Age, Travaux de la Maison de l'Orient Méditerranéen 33, Lyon, 65–83.

Freestone I.C, Leslie K.A, Thirlwall M and Gorin-Rosen Y (2003). Strontium isotopes in the investigation of early glass production: Byzantine and early Islamic glass from the Near East. Archaeometry, 45, 19–32.

Freestone I.C, Ponting M and Hughes J (2002). Origins of Byzantine glass from Maroni Petrera, Cyprus. Archaeometry, 44, 257–72. DOI: 10.1111/1475-4754.t01-1-00058

Giardino C., Pepe C (1998). I Più Antichi Vetri Della Campania. I Rinvenimenti Da Vivara (Na) Ed Il Loro Contesto Archeologico. In: Atti del convegno "Il vetro in Italia meridionale ed insulare", Napoli.

Gliozzo E (2017). The composition of colourless glass: a review. Archaeological and Anthropological Sciences June 2017, Volume 9, Issue 4, pp 455–483.

Gorgoglione M, Fiorentino G, Corridi C, Sadori L and Panetta P (1993). La capanna 7 di Torre Castelluccia (Pulsano-Taranto), dal Bronzo Finale alla prima età del Ferro. "Taras", XIII, 1-2, pp. 25-114.

Götze J and Lewis R (1994). Distribution of REE and trace elements in size and mineral fractions of high-purity quartz sands. Chemical Geology 114, 43-57.

Gratuze B (2013). Glass Characterisation Using Laser Ablation Inductively Coupled Plasma Mass Spectrometry Methods. In: Janssens K (Ed.) "Modern methods for analyzing archaeological and historical glass", John Wiley & Sons Ltd, UK. 201-234.

Gratuze B and Billaud Y (2003). La circulation des perles en verre dans le Bassin Méditerranéen, de l'Age du Bronze moyen jusqu'au Hallstatt. In: Foy D, Nenna M D (eds) Echanges et commerce du verre dans le monde antique, Montagnac: Mergoil, 11–15.

Gratuze B, Louboutin C and Billaud Y (1998). Les perles protohistoriques en verre du Musées des Antiquités nationales. Antiquités Nationales 30: 11-24.

Gratuze B and Picon M (2006). Utilisation par l'industrie verrière des sels d'aluns des oasis égyptiennes au début du premier millénaire avant notre ère. In: Brun J P. (Ed.) L'Alun de Méditerranée, Institut Français de Naples, 269-276.

Gromet L.P and Silver L.T (1983). Rare earth element distributions among minerals in a granodiorite and their petrogenetic implications. Geochimica et Cosmochimica Acta, 47, 925–39.

Guilaine J, Gratuze B. and Barrandon J.N (1990). Les perles de verre du Chalcolithique et de l'Age du Bronze. 1er Colloque de Beynac ' Le Bronze Atlantique', 10-14 Septembre 1990, Proceeding. pp. 255-266.

Hahn-Weinheimer P (1995). Spektrochemische und Physikalische Untersuchungen an latènezeitlchen Glasfunden aus dem oppidium von Manching. Beilage zum Sammelblatt des Histrorischen Vereins Ingolstadt, 65, Frankfurt-am-Main.

Hartmann G, Kappel I, Grote B and Arnold B (1997). Chemistry and technology of prehistoric glass from lower Saxony and Hesse. Journal of Archaeological Science, 24, pp. 547-559.

Henderson J (1985). The raw materials of early glass production. Oxford Journal of Archaeology, 4, pp. 267-291

Henderson J (1988a). Glass production and bronze age Europe. Antiquity 1988 62, 435-451

Henderson J (1988b). Electron probe microanalysis of mixed alkali glasses. Archaeometry 30,1, 77-91

Henderson J (1989). The scientific analysis of ancient glass and its archaeological interpretation, in: Henderson, J. (Ed.), Scientific analysis in archaeology and its interpretation. Oxford University Committee for Archaeology, Monograph no. 19, UCLA Institute of Archaeology Research Tools 5, Oxford, 30–62.

Henderson J (1993). Chemical analyses of the glass and faience from Hauterive Champreveyeres, Switzerland. In: Rychner-Faraggi A.M. (Ed.) Hauterive-Champreveyeres, 9: Metal et Parure au Bronze final, Musee cantonal d'Archaeologie, Neuchatel, 1993, pp. 111-117.

Henderson J (2000). The science and Archaeology of materials: an investigation of inorganic materials. Ed Routledge, London.

Henderson J (2013). Ancient glass, an interdisciplinary exploration. Cambridge University Press, New York.

Henderson J, Evans J, Bellintani P and Bietti-Sestieri A M. (2015). Production, mixing and provenance of Late Bronze Age mixed alkali glasses from northern Italy: an isotopic approach. Journal of Archaeological Science 55, 1-8

Jackson C.M and Nicholson P.T (2010). The provenance of some glass ingots from the Uluburun shipwreck. Journal of Archaeological Scinece, 37, 295-301. DOI: 10.1016/j.jas.2009.09.040

Jarosewich E (2002). Smithsonian microbeam standards. J. Res. NIST 107 (6), 681-685. http://www.nist.gov/jres.

Luppino S, Quondam F, Granese M.T and Vanzetti A (2010). Sibaritide. Riletture di alcuni contesti funerari tra VIII e VII secolo a.C. In: "Alle origini della Magna Grecia Mobilità migrazioni fondazioni", Atti del cinquantesimo convegno di studi sulla Magna Grecia", Taranto 1-4 ottobre 2010, pp. 643-682.

Maggiulli G (2009). I ripostigli di Roca Vecchia (Lecce): analisi dei materiali e problematiche archeologiche. In: Borgna E. Càssola Guida P. (eds.) From the Aegean to the Adriatic: social organisation, modes of exchange and interactions in postpalacial times (12th–11th BC). Proceedings of the International Conference, Udine 2oo6. Stud. Ricerche Protost. Mediterranea 8 (Roma) 239–252.

Mastroroberto M and Talamo P (2001). Il sito di Sant'Abbondio a Pompei. Continuità e trasformazione tra Bronzo Antico e Bronzo medio. In: Guzzo P.G. (ed.), Atti Pompei 2, Scienza e Società (Milano 2001), p. 208.

Mastroroberto M. (1998a) La necropoli di S. Abbondio: una comunità dell'età del Bronzo a Pompei. In: Guzzo P. G., Peroni R (eds). Archeologia e Vulcanologia in Campania. Atti del Convegno di Pompei, 21 dicembre 1996. Napoli: Arte Tipografica, 135-149.

Mastroroberto M. (1998b) La necropoli di S. Abbondio. Culto funerario a Pompei nell'età del Bronzo. In: Guzzo P. G. (ed) Pompei oltre la vita. Nuove testimonianze dalle necropoli. Pompei: Soprintendenza Archeologica di Pompei, 9-14.

Matarese I. (2016). Gli ornamenti della tomba 1 di Murgia Timone (Matera) nel quadro del Bronzo medio in Italia. In: Ornarsi per comunicare agli uomini e agli dei. Atti del XII Incontro di Studi Preistoria e Protostoria in Etruria, Manciano-Pitigliano-Valentano 12-14 settembre 2014. Milano: Centro studi di Preistoria e Archeologia, 373-386.

McKay G.A (1989). Partitioning of rare earth elements between major silicate minerals and basaltic melts. In: Lipin, B. R., and McKay, G. A. (Eds.), Geochemistry and mineralogy of rare earth elements. Reviews in Mineralogy 21, Mineralogical Society of America, Chantilly, VA, 45–77.

McLennan S.M (1989). Rare earth elements in sedimentary rocks: Influence of provenance and sedimentary processes. In: Lipin B.R. and McKay G.A. (Eds), Geochemistry and Mineralogy of REE. Mineral. Soc. Am., Rev. Mineral, 21 : 169-200.

McLune W.F (1989). Powder Diffraction File: Inorganic Phases. JCPDS International Centre for Diffraction Data, Swarthmore, PA.

Mirti P, Pace M, Negro Ponzi M.M. and Aceto M (2008). ICP-MS analysis of glass fragments of Parthian and Sasanian epoch from Seleucia and Veh Ardashir (central Iraq). Archaeometry, 50, 2008, 429-450

Nikita K and Henderson J (2006). Glass Analyses from Mycenaean Thebes and Elateia: Compositional evidence for a Mycenaean glass industry. Journal of Glass Studies, volume 48

Nolte B (1968). Die Glassgefässe im Alten Ägypten, Bruno Hessling, Berlin

Pacciarelli M. (1999). Torre Galli. La necropoli della prima età del Ferro (scavi Paolo Orsi 1922-23). Catanzaro.

Panighello S, Orsega EF, van Elteren JT, Selih VS (2012) Analysis of polychrome Iron Age glass vessels from Mediterranean I, II and III groups by LA-ICP-MS. Journal of Archaeological Sciences 39:2945–2955

Patroni G (1898). Un villaggio siculo presso Matera. MAL.

Pearce J.G, Perkins W.T, Westgate J.A, Gorton M.P, Jackson S.E, Neal C.R. and Chenery S.P (1997). A compilation of new and published major and trace element data for NIST SRM 610 and NIST SRM 612 glass reference materials. Geostand. Newsl. 21 (1), 115-144 http://dx.doi.org/10.1111/j.1751-908X.1997.tb00538.x.

Peroni R. (1994). Enotri e Micenei nella Sibaritide, 1. Trucco F (ed.) Broglio di Trebisacce.

Peroni R and Vanzetti A (2008). Broglio di Trebisacce, Guida al Parco Archeologico.

Polla A, Angelini I, Artioli G, Bellintani P, Dore A (2011) Archaeometric investigation of Early Iron Age glass from Bologna. In: Proceedings of the 37th International Symposium on Archaeometry, 13th - 16th May 2008. Siena, Italy, Springer, pp. 139–144

Purowski T, Dzierzanowski P, Bulska E, Wagner B and Nowak A (2012). A study of glass beads from the Hallstatt C–D from South-Western Poland: implications for glass technology and provenance. Archaeometry 54, 1, 144-166. DOI: 10.1111/j.1475-4754.2011.00619.x

Reade W, Freestone I.C and Bourke S (2009). Innovation and continuity in Bronze and Iron Age glass from Pella in Jordan. In: Janssens K., Degryse P., Cosyns P., Caen J. and Van't dack L. (Eds.), Annales du 17° Congrès de l'Association Internationale pour Histoire du Verre. Annales of the 17th Congress of the International Association for the History of Glass, University Press Antwerp, Antwerp, 47-54.

Reade W, Freestone I.C and Simpson S.J (2005). Innovation Or Continuity? Early First Millennium BCE Glass In The Near East: The Cobalt Blue Glasses From Assyrian Nimrud. In: Arrowsmith J.W. (Ed.), Annales du 16° Congrès de l'Association Internationale pour Histoire du Verre. Annales of the 16th Congress of the International Association for the History of Glass, Bristol, 23-27.

Rehren T (2016). Another order for glass – or: how much glass does Pharaoh need? In: Franzmeier H, Rehren Th,·Schulz R. (eds.) Mit archäologischen Schichten Geschichte schreiben Festschrift für Edgar B. Pusch zum 70. Geburtstag Forschungen in der Ramses-Stadt 10, Gerstenberg-Verlag, Hildesheim 2016 ISBN 978-3-8067-8812-9

Rehren T, Cholakova A and Zivanovic M (2012). The making of black glass in Late Roman Doclea, Montenegro. New Antique Doclea III.

Santopadre P and Verità M (2000). Analyses of the production technologies of Italian vitreous materials of the Bronze Age. Journal of Glass Studies, 42, 25-40.

Sayre E.V and Smith R.W (1961). Compositional categories of ancient glass. Science, 133, 1824–6.

Scarano T. (2012). Roca I. Le fortificazioni della media età del Bronzo. Strutture, contesti, materiali. Foggia.

Scarano T and Maggiulli G (2014). The golden sun discs from Roca Vecchia, Lecce, Italy: archaeological and cultural context. Tagungen des Landesmuseums für VorgeschichTe haLLe, Band 11.

Schlick-Nolte B and Werthmann R (2003). Glass vessels from the burial of Nesikhons. Journal of Glass Studies 45, 11-34.

Shortland A.J and Schroeder H (2009). Analysis of first millennium BC glass vessels and beads from the Pichvnari necropolis, Georgia. Archaeometry 51, 947-965. DOI:10.1111/j.1475-4754.2008.00443.x

Shortland A.J, Rogers N and Eremin K (2007). Trace element discriminants between Egyptian and Mesopotamian Late Bronze Age glasses. Journal of Archaeological Science, 34, 781–9.

Shortland A, Schachner L, Freestone I and Tite M (2006). Natron as flux in the early vitreous materials industry: sources, beginning and reasons for decline. Journal of Archaeological Science, 33, 521-530. DOI: 10.1016/j.jas.2005.09.011.

Tite M.S, Hatton G.D, Shortland A.J, Maniatis Y, Kavoussanaki D and Panagiotaki M (2005). Raw materials used to produce Aegean Bronze Age glass and related vitreous materials. In: "Annales du 16e Congrès de l'Association Internationale pour l'Histoire du verre", AIHV, Nottingham, UK, 10-13.

Tite M.S, Manti P and Shortland A.J (2007). A technological study of ancient faience from Egypt. Journal of Archaeological Science, 34, 1568-1583.

Tite M.S, Shortland A.J, Maniatis Y, Panagiotaki M and Kaczmarczyk A (2008). Faience production in the Eastern Mediterranean. In: "Production Technology of Faience and Related Early Vitreous Materials", Monograph 72, 111-128. Oxford University School of Archaeology, Oxford.

Towle A. and Henderson J (2004). The glass Bead game: archaeometric evidence for existence of an Etruscan glass Industry. Etruscan Studies, Vol. 10.

Towle A, Henderson J, Bellintani P and Gambacurta G (2001). Frattesina and Adria: report of scientific analyses of early glass from the Veneto. Padusa.

Turner W.E.S. (1956). Studies of ancient glass and glassmaking processes. Part V: Raw materials and melting processes. Journal of the Society of Glass Technology 40, 277–300.

Turner W.E.S and Rooksby H.P (1959). A study of opalising agents in ancient opal glasses throughout three thousand four hundred years. Glastechnische Berichte 32K (VII), 17–28.

Van Der Linden V, Cosyns P, Schalm O, Cagno S, Nys K, Janssens K, Nowak A, Wagner B and Bulska E (2009). Deeply coloured and black glass in the northern provinces of the roman empire: differences and similarities in chemical composition before and after ad 150*. Archaeometry, 51, 5, 822–844. DOI: 10.1111/j.1475-4754.2008.00434.x

Varberg J, Gratuze B and Kaul F (2015). Between Egypt, Mesopotamia and Scandinavia: Late Bronze Age glass beads found in Denmark. Journal of Archaeological Science 54, 168-181.

Varberg J, Gratuze B, Kaul F, Hansen A H, Rotea M and Wittenberger M (2016). Mesopotamian glass from Late Bronze Age Egypt, Romania, Germany, and Denmark. Journal of Archaeological Science 74, 184-194. https://doi.org/10.1016/j.jas.2016.04.010

Venclová N, Hulínský V, Henderson J, Chenery S, Šulová L and Hložek J (2011). Late Bronze Age mixed-alkali glasses from Bohemia. Archeologické rozhledy LXIII

Walton M.S, Shortland A, Kirk S. and Degryse P (2009). Evidence for the trade of Mesopotamian and Egyptian glass to Mycenaean Greece. Journal of Archaeological Science vol. 36, 1496-1503

Wedepohl K. H and Baumann A (2000). The use of marine molluskan shells for Roman glass and local raw glass production in the Eifel area (Western Germany). Naturwissenschaften, 87, 129–32.

Wedepohl K. H, Simon K and Kronz A (2011a). Data on 61 chemical elements for the characterization of three major glass compositions in Late Antiquity and the Middle Ages. Archaeometry, 53, 81–102.

Wedepohl K. H, Simon K and Kronz A (2011b). The chemical composition including the Rare Earth Elements of the three major glass types of Europe and the Orient used in late antiquity and the Middle Ages. Chemie der Erde, 71, 289–96. DOI: 10.16/j.chemer.2011.04.001

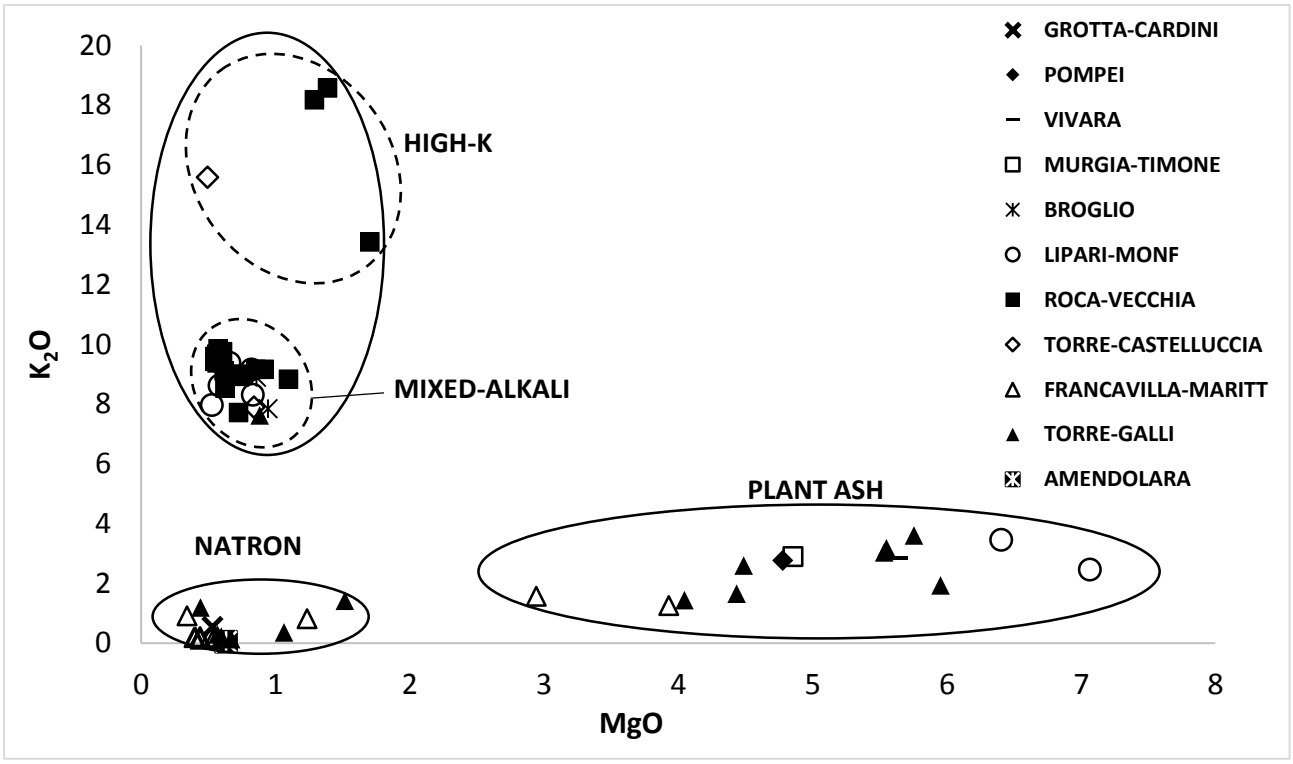


Fig. 1. $K_2O$ vs. MgO (weight %) for the analysed samples.

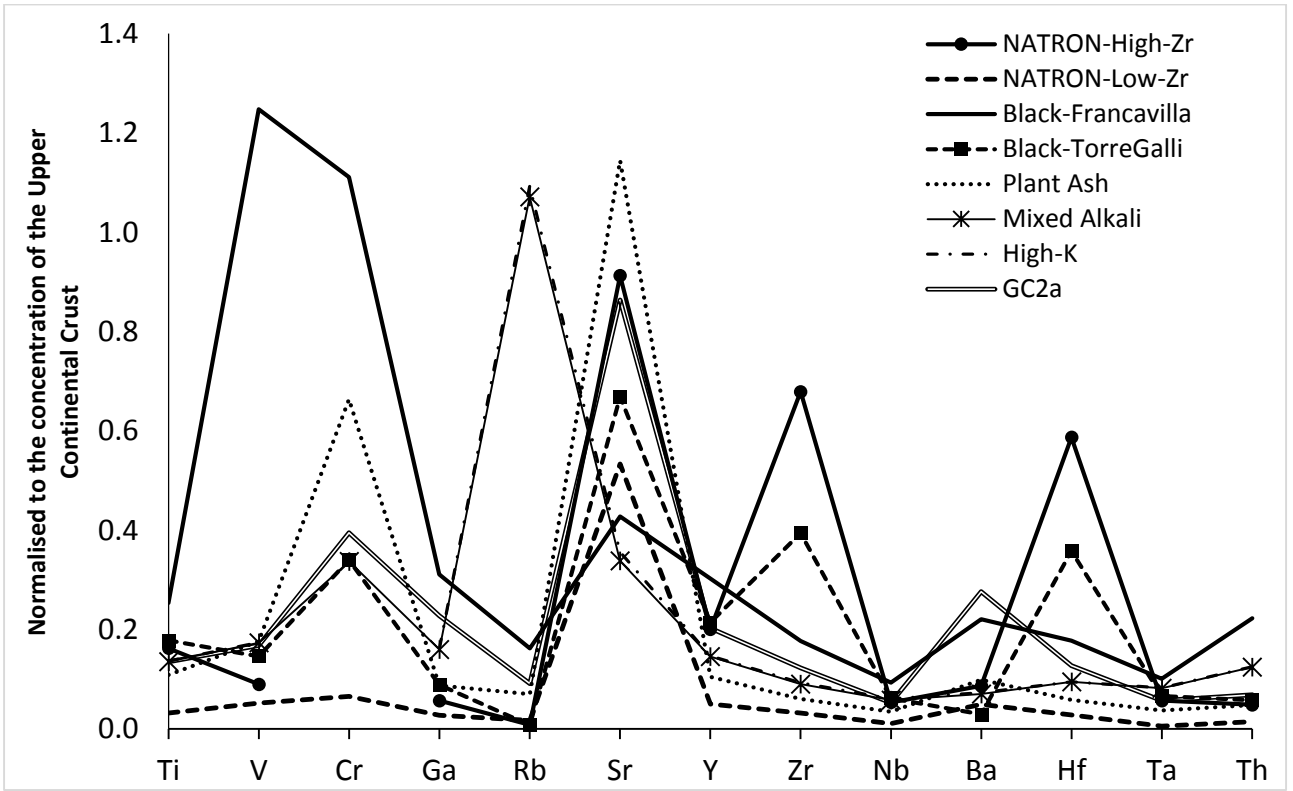


Fig. 2. Average trace-element composition of all glass groups, normalised to the composition of the upper continental crust (Wedepohl 1995).

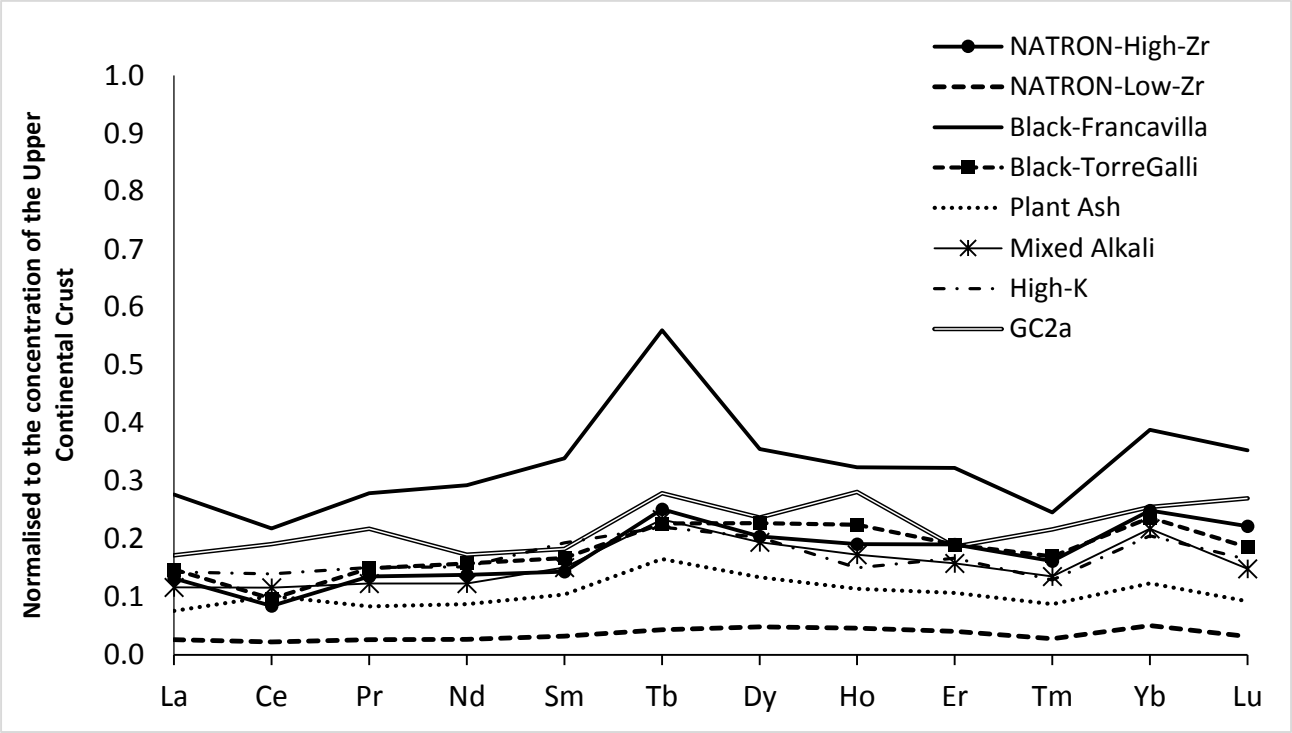


Fig. 3 Average REEs composition of all glass groups, normalised to the composition of the upper continental crust (Wedepohl 1995).

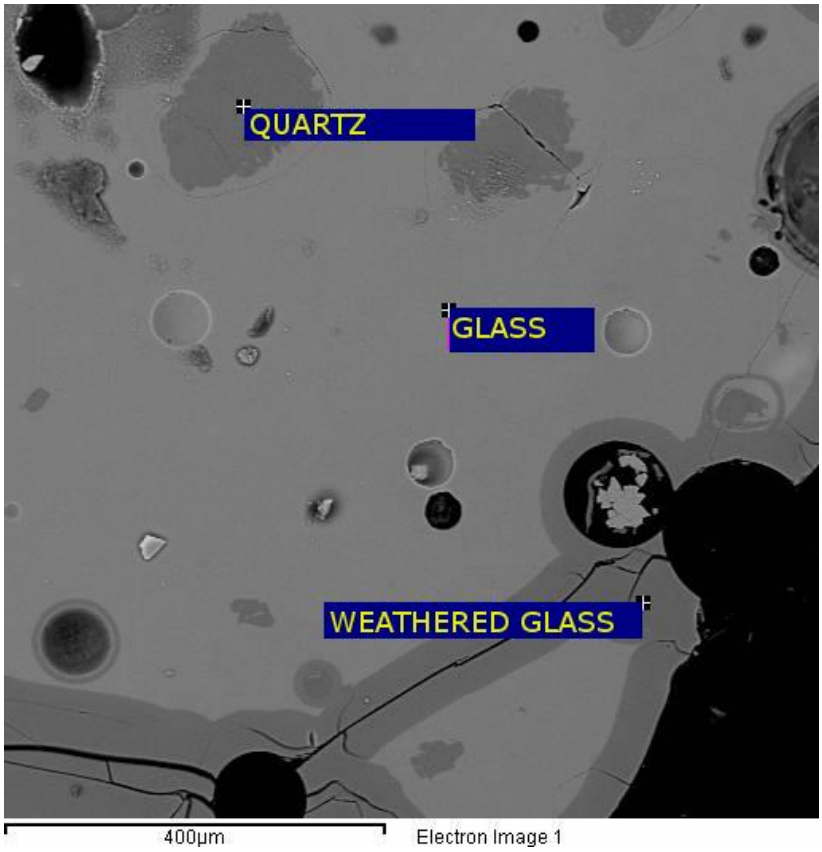


Fig. 4 Back-scattered electron (BSE) image of sample RC2b3.

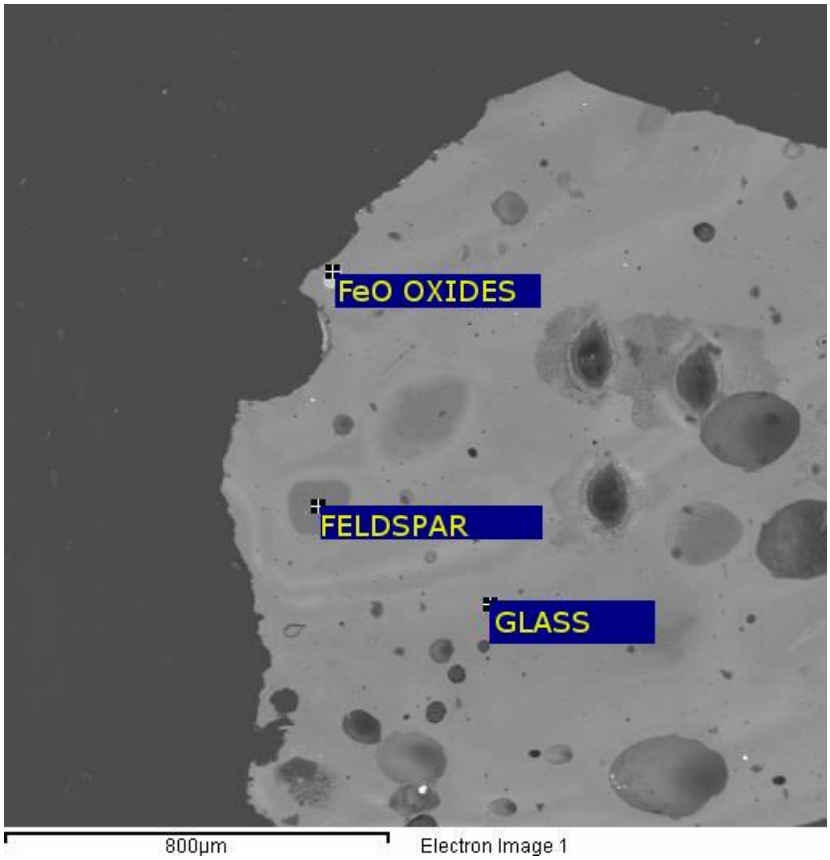


Fig. 5 Back-scattered electron (BSE) image of sample FM7bl.

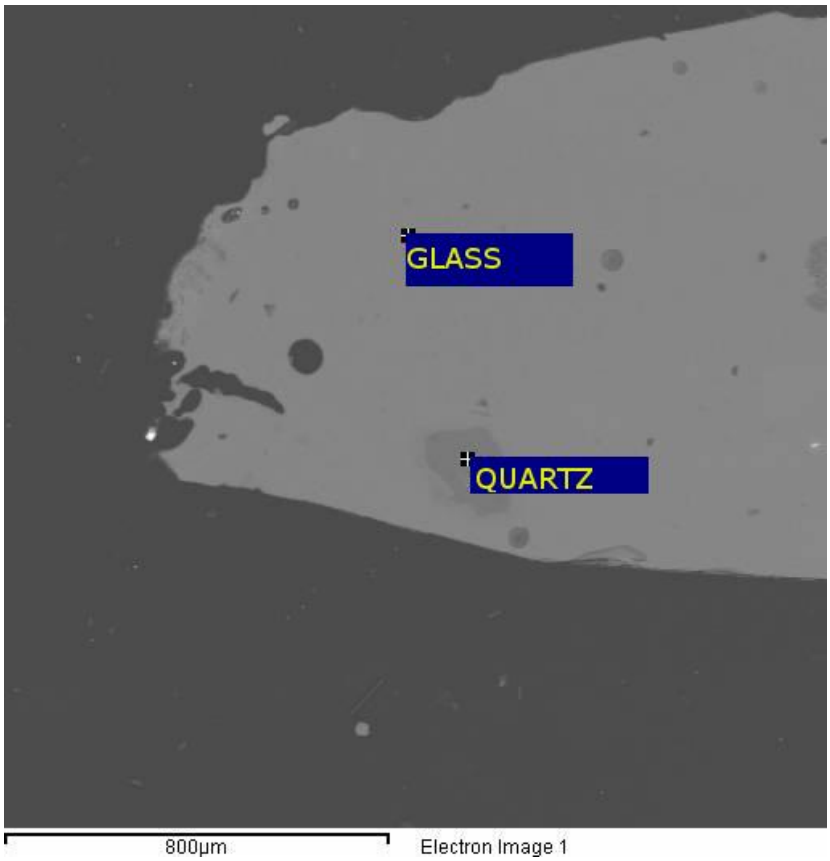


Fig. 6 Back-scattered electron (BSE) image of sample TG13bl.

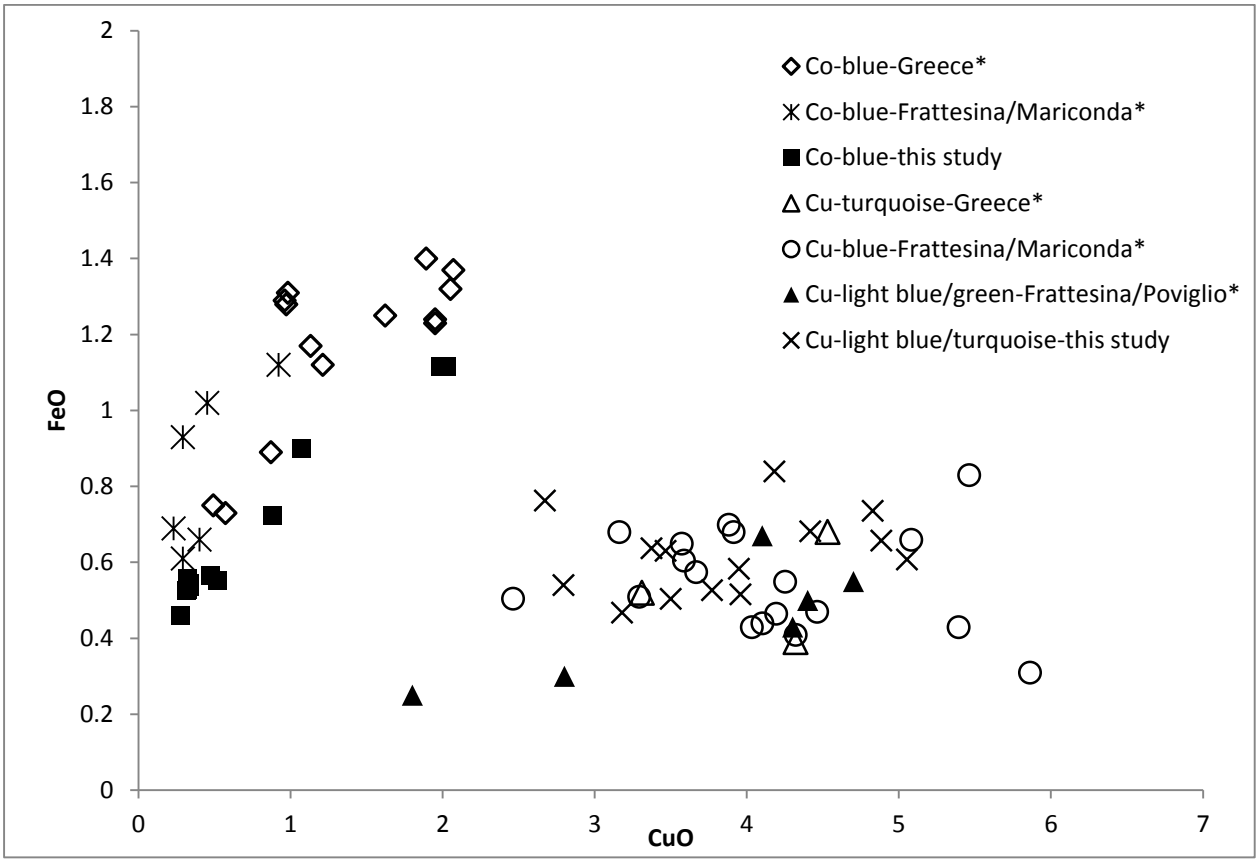


Fig. 7 FeO vs. CuO values of Mixed Alkali samples coming from Italy (Frattesina/Maricorda – Towle et al. 2001; Frattesina/Poviglio – Santopadre and Verità 2000), Greece (Nikita and Henderson 2006) and this study.

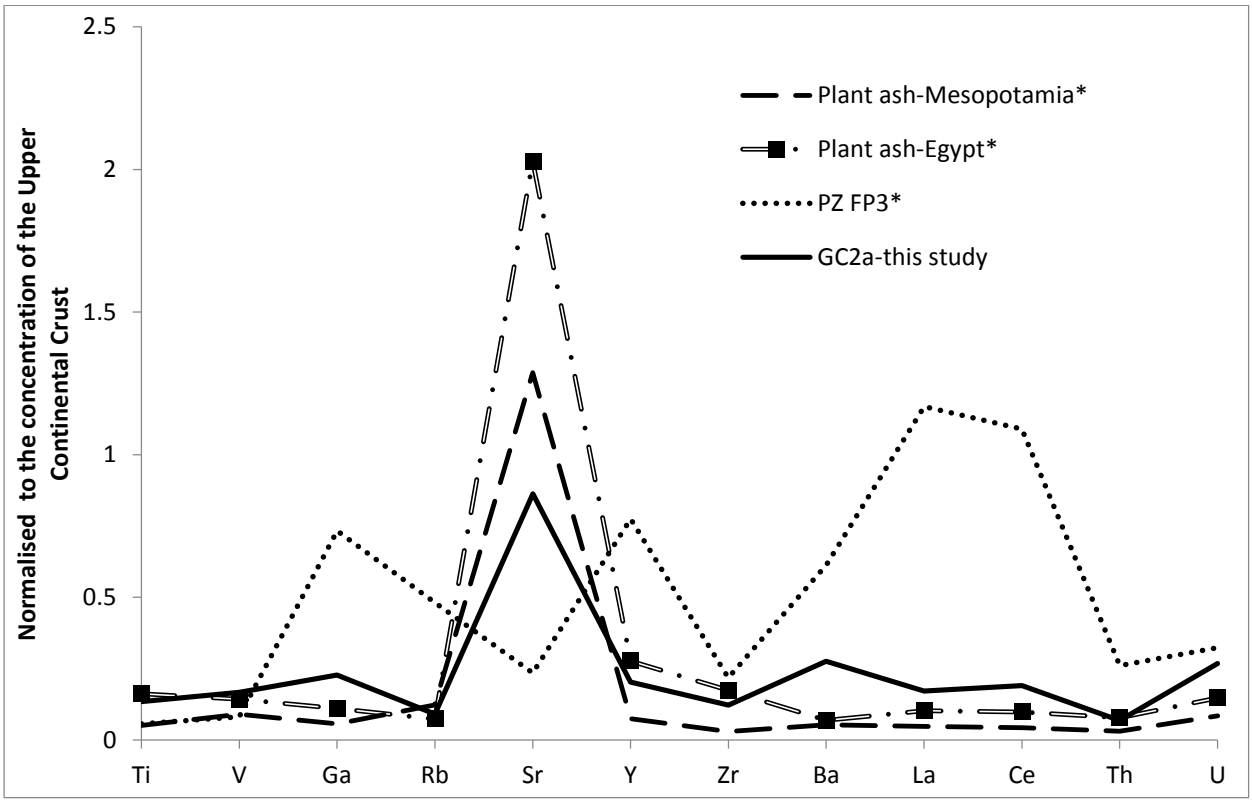


Fig. 8 Trace-element composition of GC2a sample of this study, compared to LMLK samples from Punta di Zambrone (Conte et al. 2015) and Plant Ash glass produced in Egypt and Mesopotamia (Shortland et al. 2007). Normalised to the composition of the upper continental crust (Wedepohl, 1995).

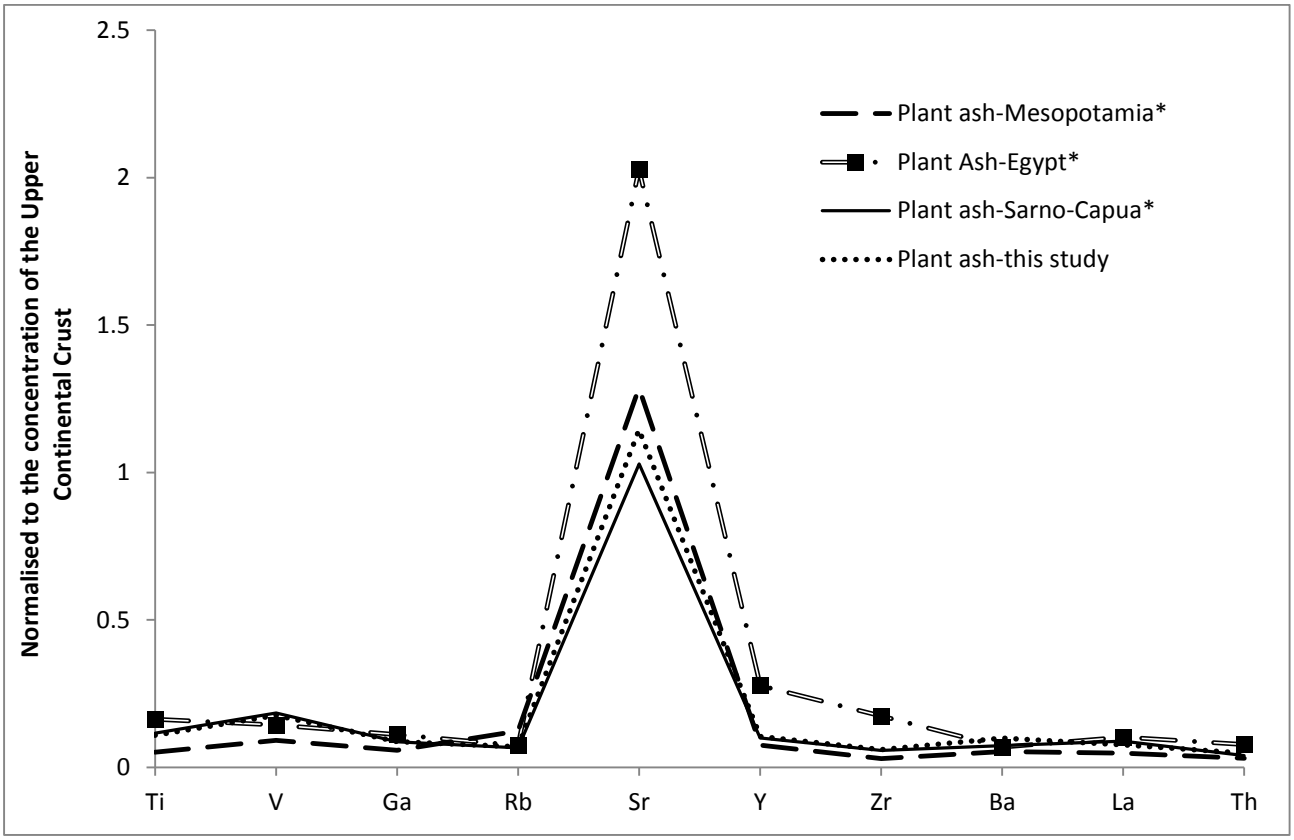


Fig. 9. Trace-element composition of Plant Ash glass of this study, compared to glass found in Italy (Sarno-Capua, Conte et al. 2016a) and glass produced in Egypt and Mesopotamia (Shortland et al. 2007). Normalised to the composition of the upper continental crust (Wedepoh, 1995).

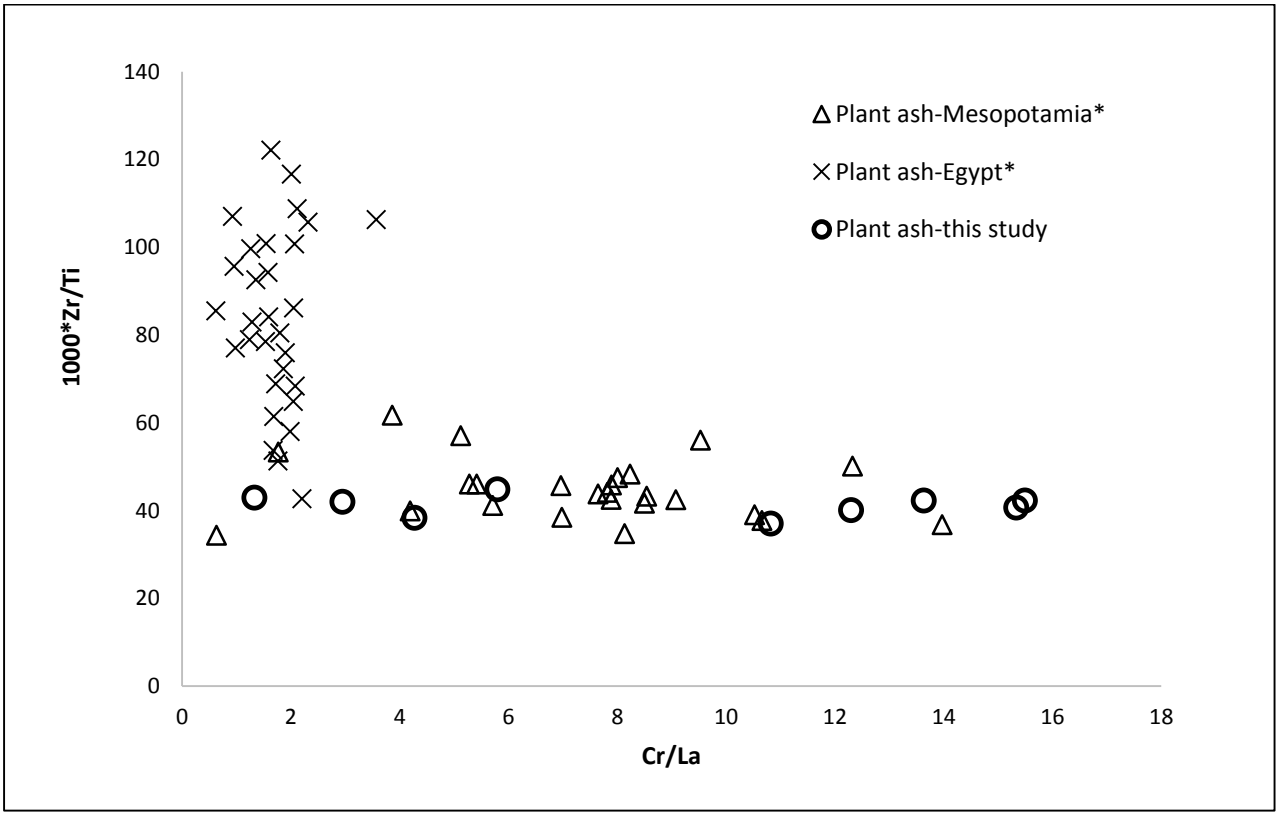


Fig. 10. Zr/Ti *vs.* Cr/La ratios of Plant Ash glass produced in Egypt and Mesopotamia (Shortland et al. 2007) and this study.

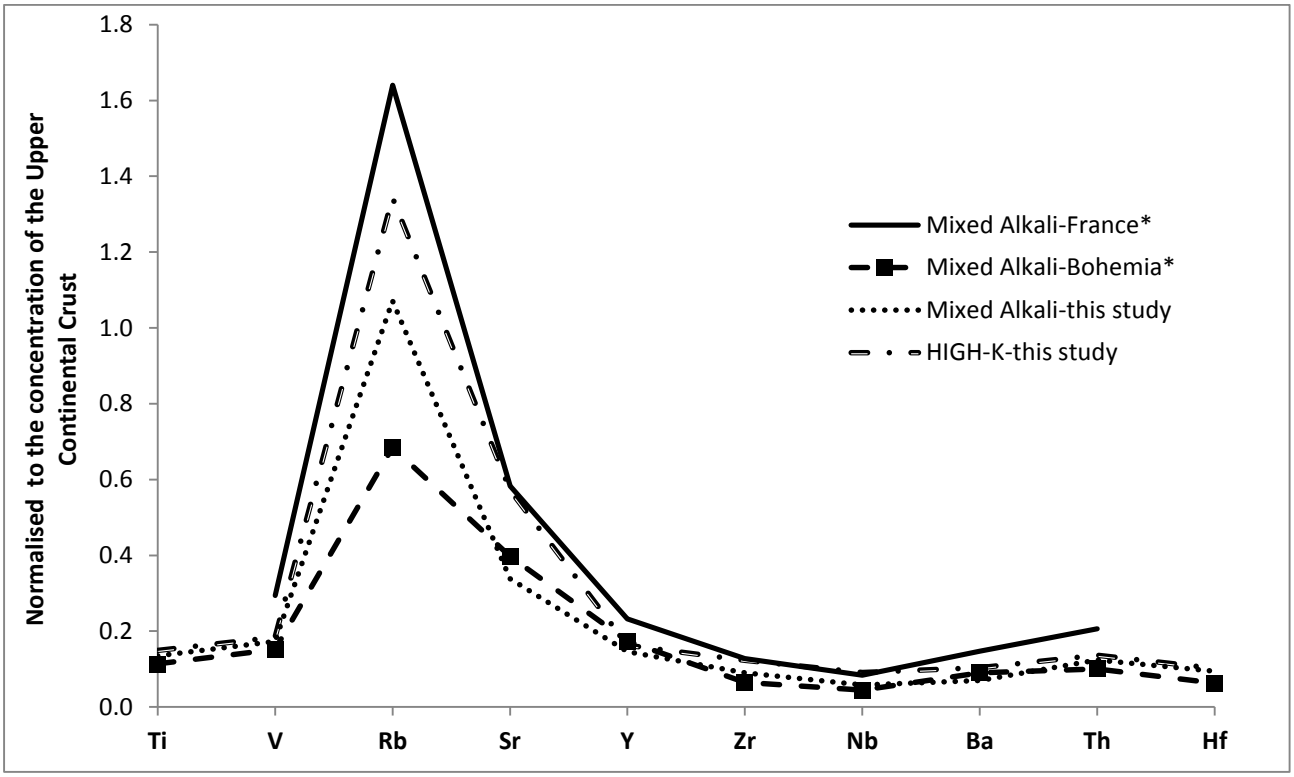


Fig. 11. Trace element composition of Mixed alkali and High-K samples of this study, compared to LMHK glass coming from France (Croutsch et al. 2011) and Bohemia (Venclovà et al. 2011). Normalized to the composition of the upper continental crust (Wedepohl 1995).

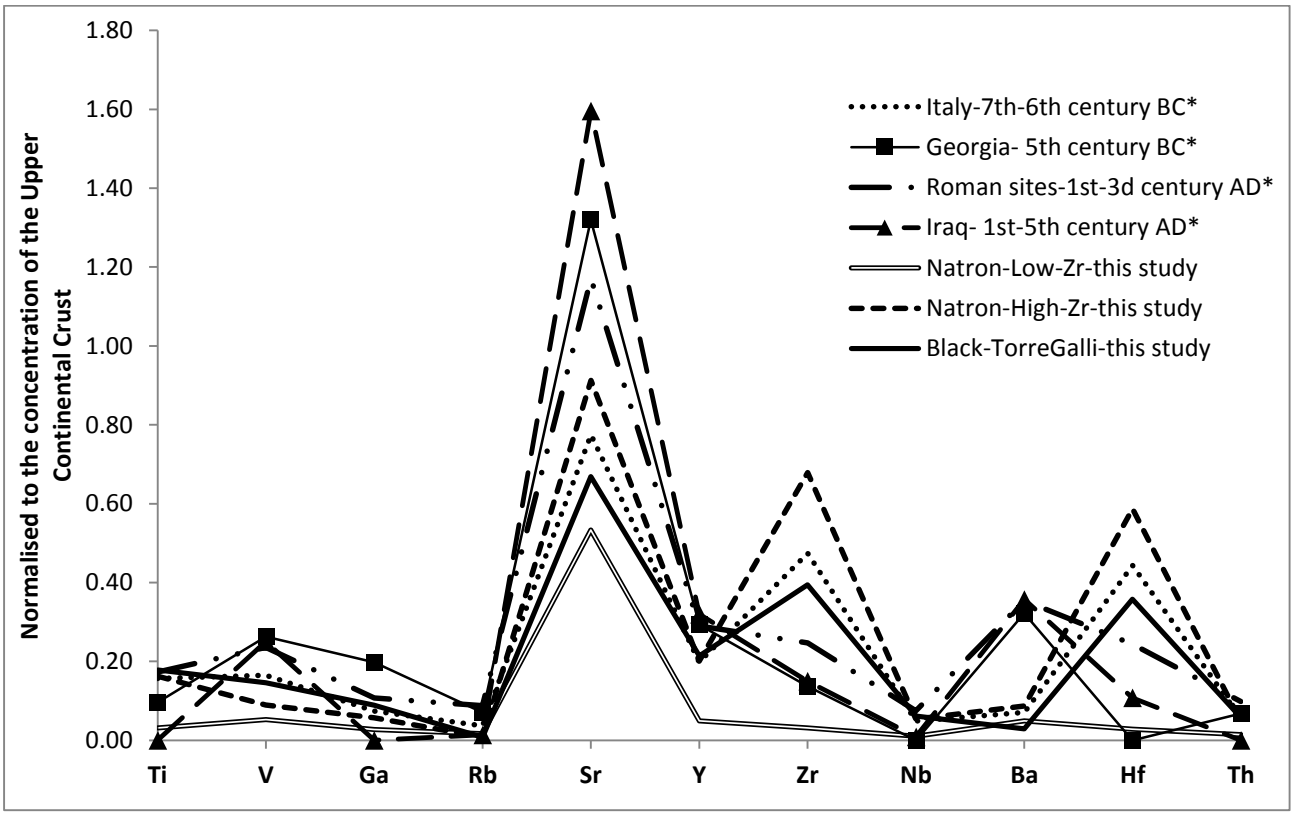


Fig. 12. Trace element composition of Natron samples of this study (included black glass from Torre Galli), compared to natron glass coming from Italy – 7$^{th}$-6$^{th}$ century BC (Conte et al. 2016a), Georgia- 5$^{th}$ century BC (Shortland and Schroeder 2009), Roman sites -1$^{st}$-3$^{rd}$ century AD (Degryse and Shortland 2009) and Central Iraq -1$^{st}$-5$^{th}$ century AD (Mirti et al. 2008). Normalized to the composition of the upper continental crust (Wedepohl 1995).

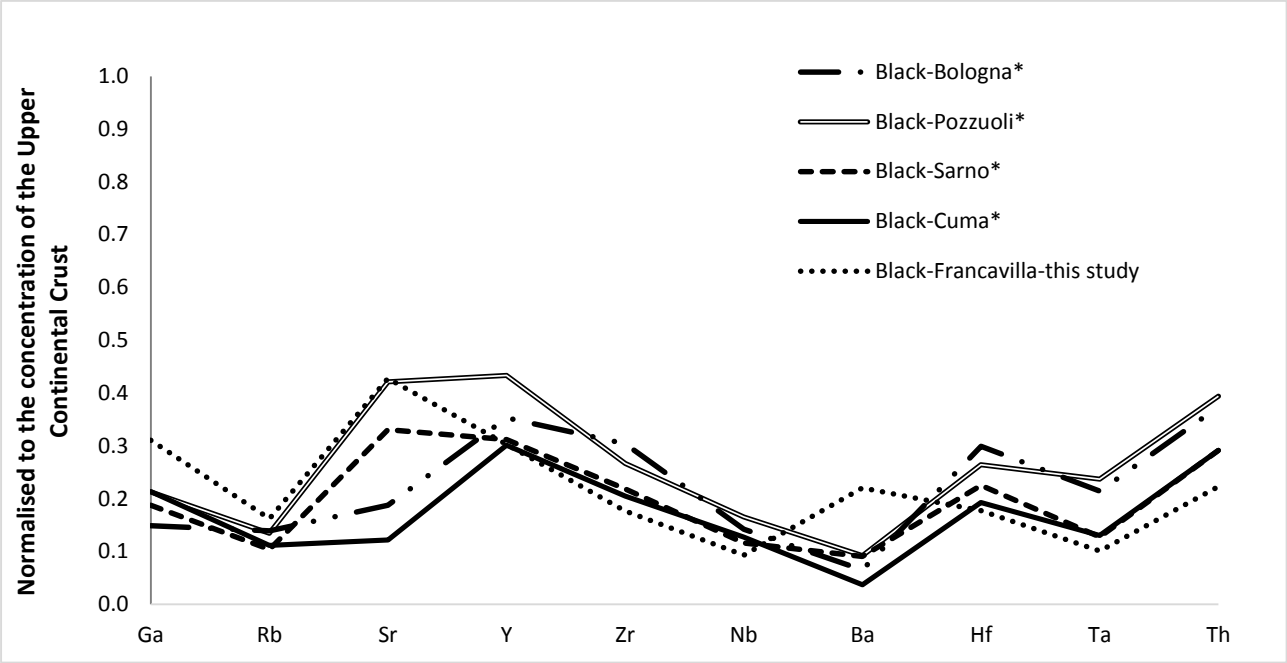


Fig. 13. Trace element composition of black glass from Francavilla Marittima of this study, compared to black glass coming from Sarno, Cuma, Pozzuoli and Bologna (Conte et al. 2016a, b). Normalized to the composition of the upper continental crust (Wedepohl 1995).

Table 1

| Sample | Site | Context | Material | Description | Colour | Opacity | Chronology | Century |
|---|---|---|---|---|---|---|---|---|
| **GC2a** | Grotta Cardini | Tomb area B | glass | flattened-globular bead | amber | no | Eneolithic-EBA | 22$^{th}$-18$^{th}$ BC |
| **PM1g** | Pompei-S. Abbondio | Tomb 26R | faience | segmented cylindrical bead | green | yes | EBA | 18$^{th}$-17$^{th}$ cent BC |
| **V1l** | Vivara | Punta D'Alaca - "Fossa Alpha" | glass | globular bead | light-blue | no | MBA2 | End 16$^{th}$-15$^{th}$ cent BC |
| **MT2t** | Murgia Timone | Tomb 1 | glass | flattened-globular bead | light-blue | no | MBA3 | End 15$^{th}$-14$^{th}$ cent BC |
| **BDT1l** | Broglio di Trebisacce | Village-Trench 2 | glass | barrel ligh-blue bead with spiral white decoration | ligh-blue | no | FBA | End 12$^{th}$-10$^{th}$ cent BC |
| **BDT1w** | Broglio di Trebisacce | Village-Trench 2 | glass | barrel ligh-blue bead with spiral white decoration | white | yes | FBA | End 12$^{th}$-10$^{th}$ cent BC |
| **MON1b** | Lipari-P. Monfalcone | Tomb 18 | glass | discoidal bead | blue | no | FBA | End 12$^{th}$-11$^{th}$ cent BC |
| **MON2b** | Lipari-P. Monfalcone | Tomb 31 | glass | discoidal bead | blue | no | FBA | End 12$^{th}$-11$^{th}$ cent BC |
| **MON3g** | Lipari-P. Monfalcone | Tomb 31 | glass | discoidal bead | green | no | FBA | End 12$^{th}$-11$^{th}$ cent BC |
| **MON4l** | Lipari-P. Monfalcone | Tomb 31 | glass | discoidal bead | light-blue | no | FBA | End 12$^{th}$-11$^{th}$ cent BC |
| **MON5l** | Lipari-P. Monfalcone | Tomb 31 | glass | discoidal bead | light-blue | no | FBA | End 12$^{th}$-11$^{th}$ cent BC |
| **MON6g** | Lipari-P. Monfalcone | Tomb 31 | glass | discoidal bead | green | no | FBA | End 12$^{th}$-11$^{th}$ cent BC |
| **MON7l** | Lipari-P. Monfalcone | Tomb 31 | glass | discoidal bead | light-blue | no | FBA | End 12$^{th}$-11$^{th}$ cent BC |
| **RC2b1** | Roca Vecchia | "Ripostiglio degli Ori" | glass | discoidal bead | blue | no | FBA | End 12$^{th}$-10$^{th}$ cent BC |
| **RC2b2** | Roca Vecchia | "Ripostiglio degli Ori" | glass | discoidal bead | blue | no | FBA | End 12$^{th}$-10$^{th}$ cent BC |
| **RC2b3** | Roca Vecchia | "Ripostiglio degli Ori" | glass | discoidal bead | blue | no | FBA | End 12$^{th}$-10$^{th}$ cent BC |
| **RC3b1** | Roca Vecchia | "Ripostiglio degli Ori" | glass | discoidal bead | blue | no | FBA | End 12$^{th}$-10$^{th}$ cent BC |
| **RC3b2** | Roca Vecchia | "Ripostiglio degli Ori" | glass | discoidal bead | blue | no | FBA | End 12$^{th}$-10$^{th}$ cent BC |
| **RC4t** | Roca Vecchia | "Ripostiglio degli Ori" | glass | discoidal bead | turquoise | no | FBA | End 12$^{th}$-10$^{th}$ cent BC |
| **RC6g** | Roca Vecchia | "Ripostiglio degli Ori" | glass | discoidal bead | green | no | FBA | End 12$^{th}$-10$^{th}$ cent BC |
| **RC7g** | Roca Vecchia | "Ripostiglio degli Ori" | glass | discoidal bead | green | no | FBA | End 12$^{th}$-10$^{th}$ cent BC |

| Sample | Site | Context | Material | Description | Colour | Opacity | Chronology | Century |
|---|---|---|---|---|---|---|---|---|
| **RC8b** | Roca Vecchia | "Ripostiglio degli Ori" | glass | discoidal bead | blue | no | FBA | End 12th-10th cent BC |
| **RC11b** | Roca Vecchia | "Ripostiglio degli Ori" | glass | discoidal bead | blue | no | FBA | End 12th-10th cent BC |
| **RC12b** | Roca Vecchia | "Ripostiglio degli Ori" | glass | discoidal bead | blue | no | FBA | End 12th-10th cent BC |
| **RC13b** | Roca Vecchia | "Ripostiglio degli Ori" | glass | discoidal bead | blue | no | FBA | End 12th-10th cent BC |
| **RC14t** | Roca Vecchia | "Ripostiglio degli Ori" | glass | turquoise four-horned bead with white rings on the horns (eyes bead) | turquoise | no | FBA | End 12th-10th cent BC |
| **RC14w** | Roca Vecchia | "Ripostiglio degli Ori" | glass | turquoise four-horned bead with white rings on the horns (eyes bead) | white | yes | FBA | End 12th-10th cent BC |
| **RC15t** | Roca Vecchia | "Ripostiglio degli Ori" | glass | turquoise four-horned bead with white rings on the horns (eyes bead) | turquoise | no | FBA | End 12th-10th cent BC |
| **RC15w** | Roca Vecchia | "Ripostiglio degli Ori" | glass | turquoise four-horned bead with white rings on the horns (eyes bead) | white | yes | FBA | End 12th-10th cent BC |
| **RC16l** | Roca Vecchia | "Ripostiglio degli Ori" | glass | light-blue four-horned bead with white rings on the horns (eyes bead) | light-blue | no | FBA | End 12th-10th cent BC |
| **RC17t** | Roca Vecchia | "Ripostiglio degli Ori" | glass | turquoise four-horned bead with white rings on the horns (eyes bead) | turquoise | no | FBA | End 12th-10th cent BC |
| **RC18t** | Roca Vecchia | "Ripostiglio degli Ori" | glass | flattened-globular bead | turquoise | no | FBA | End 12th-10th cent BC |
| **RC20g** | Roca Vecchia | "Ripostiglio degli Ori" | glass | discoidal bead | green | ? | FBA | End 12th-10th cent BC |
| **TC1l** | Torre Castelluccia | "Lumber-room" - Hut 7 | glass | discoidal bead | light-blue | no | FBA | End 12th-10th cent BC |
| **TC3l** | Torre Castelluccia | "Lumber-room" - Hut 7 | glass | discoidal bead | blue | no | FBA | End 12th-10th cent BC |
| **TG1l** | Torre Galli | Tomb 53 | glass | light-blue polylobated bead, with white eyes (eyes bead) | light-blue | no | EIA1 | 9th cent BC |
| **TG3bl** | Torre Galli | Tomb 325 | glass | black slightly triangular flattened-globular bead, with white rings at the corners (eyes bead) | black | no | O/A | 7th-6th cent BC |
| **TG5l** | Torre Galli | Tomb 313 | glass | discoidal bead | light-blue | no | EIA1 | 9th cent BC |
| **TG7inc** | Torre Galli | Tomb 158 | glass | polylobated bead | colourless | no | EIA1 | 9th cent BC |
| **TG8l** | Torre Galli | Tomb 199 | glass | barrel bead | light-blue | no | EIA1 | 9th cent BC |
| **TG9l** | Torre Galli | Tomb 231 | glass | globular bead | light-blue | no | EIA1 | 9th cent BC |
| **TG10l** | Torre Galli | Tomb 181 | glass | fragment of an eyes bead? | light-blue | no | EIA1 | 9th cent BC |
| **TG11bl** | Torre Galli | Tomb 53 | glass | globular bead decorated with chevrons | black | no | EIA1 | 9th cent BC |

| Sample | Site | Context | Material | Description | Colour | Opacity | Chronology | Century |
|---|---|---|---|---|---|---|---|---|
| **TG12bl** | Torre Galli | Tomb 3 | glass | cylindrical black bead with spiral white decoration | black | no | O/A | 7th-6th cent BC |
| **TG12w** | Torre Galli | Tomb 3 | glass | cylindrical black bead with spiral white decoration | white | yes | O/A | 7th-6th cent BC |
| **TG13bl** | Torre Galli | Tomb 12 | glass | black eyes flattened-globular bead, whit white eyes | black | no | O/A | 7th-6th cent BC |
| **TG13w** | Torre Galli | Tomb 12 | glass | black eyes flattened-globular bead, whit white eyes | white | yes | O/A | 7th-6th cent BC |
| **TG14l** | Torre Galli | Tomb 67 | glass | barrel bead | light-blue | no | EIA1 | 9th cent BC |
| **TG17l** | Torre Galli | Tomb 45 | glass | light-blue four-horned bead | light-blue | no | EIA1 | 9th cent BC |
| **FM2y** | Francavilla | Tomb 8 Temparella | glass | pear-shaped pendant | yellow | yes | EIA2 | 8th cent BC |
| **FM3inc** | Francavilla | Tomb 67 | glass | globular bead | colourless | no | EIA2 | 8th cent BC |
| **FM4inc** | Francavilla Marittima | Tomb 59 | glass | discoidal bead | colourless/light-green | no | EIA2 | 8th cent BC |
| **FM5a** | Francavilla Marittima | Tomb 65 | glass | discoidal bead | amber | no | EIA2 | 8th cent BC |
| **FM6l** | Francavilla Marittima | Tomb 61/62 | glass | discoidal bead | light-blue | no | EIA2 | 8th cent BC |
| **FM7bl** | Francavilla Marittima | Tomb 8 | glass | flower-shaped pendant with yellow edges | black | no | EIA2 | 8th cent BC |
| **FM8bl** | Francavilla Marittima | Tomb 61/62 | glass | black ribbed cylindrical bead whit yellow spiral decoration | black | no | EIA2 | 8th cent BC |
| **FM8y** | Francavilla Marittima | Tomb 61/62 | glass | black ribbed cylindrical bead whit yellow spiral decoration | yellow | yes | EIA2 | 8th cent BC |
| **FM9y** | Francavilla Marittima | Tomb 84 | glass | blue spindle whorl with yellow and white decorations | yellow | yes | EIA2 | 8th cent BC |
| **FM10a** | Francavilla Marittima | Tomb 73 | glass | flattened-globular bead | amber | no | O | 7th cent BC |
| **FM11a** | Francavilla Marittima | Tomb V6 Vigneto | glass | big discoidal bead | amber | no | EIA2 | 8th cent BC |
| **AM1g** | Amendolara | Tomb 60/60 bis, Paladino Ovest | glass | biconical bead | green | no | O/A | 7th-6th sec BC |

Table 1 Summary table of the analysed samples: site, context, material, description, colour, opacity, chronology, century. The samples removed from the same object are indicated by the same label, with the addition of the last letter(s), indicating the colour (e.g: white=w, black=bl, …)

Table 2

| Sample | Chemical type | $Na_2O$ | MgO | $Al_2O_3$ | $SiO_2$ | $P_2O_5$ | $SO_3$ | Cl | $K_2O$ | CaO | $TiO_2$ | MnO | FeO | CoO | $Cu_2O$ | $SnO_2$ | $Sb_2O_3$ | PbO | Totals |
|---|---|---|---|---|---|---|---|---|---|---|---|---|---|---|---|---|---|---|---|
| **GC2a** | **LMLK** | 12,54 | 0,53 | 3,18 | 74,78 | 0,05 | 0,09 | 0,96 | 0,56 | 6,75 | 0,10 | 0,02 | 0,49 | 0,01 | 0,01 | 0,01 | bdl | 0,04 | 100,09 |
| **PM1g** | **PLANT ASH** | 18,13 | 4,78 | 0,62 | 65,39 | 0,34 | 0,32 | 1,25 | 2,78 | 6,16 | 0,06 | 0,20 | 0,38 | bdl | 0,95 | 0,06 | 0,02 | 0,05 | 101,49 |
| **V1l** | **PLANT ASH** | 18,12 | 5,64 | 1,30 | 64,48 | 0,28 | 0,26 | 1,00 | 2,85 | 4,86 | 0,07 | 0,04 | 0,51 | 0,01 | 1,22 | 0,01 | 0,01 | 0,05 | 100,70 |
| **MT2t** | **PLANT ASH** | 13,86 | 4,85 | 0,63 | 70,21 | 0,19 | 0,28 | 0,73 | 2,91 | 5,82 | 0,03 | 0,03 | 0,29 | 0,01 | 1,12 | 0,02 | 0,01 | 0,01 | 101,00 |
| **MON3g** | **PLANT ASH** | 18,42 | 6,40 | 1,20 | 62,06 | 0,31 | 0,74 | 1,12 | 3,47 | 7,28 | 0,09 | 0,05 | 0,84 | 0,01 | 0,04 | 0,02 | 0,04 | bdl | 102,08 |
| **MON6g** | **PLANT ASH** | 20,66 | 7,06 | 0,91 | 61,12 | 0,30 | 0,42 | 0,86 | 2,47 | 6,59 | 0,07 | 0,04 | 0,51 | bdl | 0,67 | 0,01 | bdl | bdl | 101,70 |
| **FM3inc** | **PLANT ASH** | 15,16 | 3,93 | 0,81 | 71,01 | 0,30 | 0,19 | 0,83 | 1,26 | 7,47 | 0,09 | 0,02 | 0,53 | 0,01 | bdl | 0,01 | 0,05 | 0,02 | 101,68 |
| **FM6l** | **PLANT ASH** | 15,75 | 2,94 | 0,73 | 70,87 | 0,33 | 0,24 | 0,78 | 1,57 | 8,04 | 0,06 | 0,03 | 0,46 | 0,02 | 1,10 | 0,04 | 0,01 | 0,06 | 103,04 |
| **TG5l** | **PLANT ASH** | 17,02 | 5,53 | 1,21 | 65,70 | 0,24 | 0,30 | 0,77 | 3,04 | 5,12 | 0,07 | 0,05 | 0,52 | bdl | 1,22 | 0,02 | 0,01 | bdl | 100,81 |
| **TG7inc** | **PLANT ASH** | 20,95 | 5,95 | 0,65 | 64,11 | 0,28 | 0,31 | 1,23 | 1,94 | 5,59 | 0,11 | 0,03 | 0,39 | bdl | bdl | 0,01 | bdl | 0,06 | 101,61 |
| **TG8l** | **PLANT ASH** | 19,66 | 4,43 | 0,74 | 66,56 | 0,28 | 0,31 | 1,21 | 1,66 | 5,75 | 0,10 | 0,09 | 0,50 | 0,01 | 0,90 | 0,06 | 0,04 | 0,10 | 102,40 |
| **TG9l** | **PLANT ASH** | 17,72 | 4,05 | 1,08 | 67,36 | 0,34 | 0,19 | 1,32 | 1,44 | 6,66 | 0,13 | 0,30 | 0,69 | bdl | 1,03 | 0,01 | bdl | 0,01 | 102,33 |
| **TG10l** | **PLANT ASH** | 18,12 | 5,55 | 1,12 | 62,62 | 0,38 | 0,43 | 0,48 | 3,18 | 7,11 | 0,08 | 0,04 | 0,56 | bdl | 1,20 | 0,01 | 0,02 | bdl | 100,91 |
| **TG14l** | **PLANT ASH** | 19,50 | 4,49 | 0,37 | 65,85 | 0,39 | 0,31 | 1,17 | 2,61 | 6,28 | 0,07 | 0,05 | 0,22 | bdl | 0,88 | 0,02 | 0,01 | 0,05 | 102,27 |
| **TG17l** | **PLANT ASH** | 18,01 | 5,75 | 1,26 | 61,43 | 0,42 | 0,44 | 0,40 | 3,62 | 7,70 | 0,08 | 0,04 | 0,58 | 0,01 | 0,99 | 0,01 | 0,02 | 0,06 | 100,83 |
| **BDT1l** | **MIXED ALKALI** | 7,80 | 0,86 | 1,79 | 74,01 | 0,32 | 0,06 | 0,18 | 8,91 | 1,88 | 0,08 | 0,01 | 0,64 | 0,01 | 3,37 | 0,17 | 0,05 | 0,04 | 100,18 |
| **BDT1w** | **MIXED ALKALI** | 6,42 | 0,94 | 2,28 | 78,44 | 0,14 | 0,01 | 0,45 | 7,85 | 4,75 | 0,07 | 0,01 | 0,66 | bdl | 0,38 | bdl | 0,02 | 0,01 | 102,44 |
| **MON1b** | **MIXED ALKALI** | 6,85 | 0,82 | 1,65 | 77,21 | 0,28 | 0,01 | 0,04 | 9,18 | 1,72 | 0,07 | 0,02 | 0,72 | 0,11 | 0,88 | 0,05 | 0,21 | 0,04 | 99,85 |
| **MON2b** | **MIXED ALKALI** | 7,11 | 0,83 | 2,09 | 73,67 | 0,25 | 0,04 | 0,13 | 8,32 | 2,13 | 0,09 | 0,02 | 1,12 | 0,08 | 2,03 | 0,02 | 0,38 | 0,14 | 98,47 |
| **MON4l** | **MIXED ALKALI** | 7,52 | 0,58 | 2,10 | 75,04 | 0,24 | 0,02 | 0,10 | 8,64 | 1,86 | 0,09 | 0,01 | 0,63 | 0,01 | 3,46 | 0,01 | 0,06 | bdl | 100,36 |
| **MON5l** | **MIXED ALKALI** | 7,74 | 0,52 | 2,03 | 74,27 | 0,26 | 0,04 | 0,11 | 7,98 | 1,84 | 0,06 | 0,01 | 0,50 | 0,01 | 3,50 | 0,06 | 0,07 | 0,02 | 99,02 |
| **MON7l** | **MIXED ALKALI** | 7,50 | 0,65 | 1,54 | 76,57 | 0,17 | 0,02 | 0,07 | 9,39 | 1,13 | 0,08 | bdl | 0,54 | 0,01 | 2,79 | 0,16 | 0,07 | 0,03 | 100,73 |
| **RC2b1** | **MIXED ALKALI** | 6,76 | 0,55 | 1,31 | 77,58 | 0,18 | 0,02 | 0,07 | 9,58 | 1,44 | 0,06 | 0,02 | 0,53 | 0,12 | 0,31 | 0,03 | 0,25 | 0,02 | 98,82 |
| **RC2b2** | **MIXED ALKALI** | 6,97 | 0,56 | 1,41 | 77,51 | 0,18 | 0,02 | 0,04 | 9,39 | 1,52 | 0,06 | 0,01 | 0,56 | 0,12 | 0,47 | bdl | 0,29 | 0,05 | 99,18 |
| **RC2b3** | **MIXED ALKALI** | 6,73 | 0,56 | 1,37 | 77,40 | 0,19 | 0,02 | 0,07 | 9,67 | 1,49 | 0,06 | 0,02 | 0,53 | 0,12 | 0,32 | bdl | 0,26 | 0,02 | 98,83 |
| **RC3b1** | **MIXED ALKALI** | 6,80 | 0,55 | 1,28 | 77,41 | 0,15 | 0,02 | 0,06 | 9,60 | 1,47 | 0,05 | 0,01 | 0,54 | 0,12 | 0,34 | 0,01 | 0,27 | 0,02 | 98,71 |
| **RC3b2** | **MIXED ALKALI** | 6,86 | 0,55 | 1,35 | 77,54 | 0,19 | 0,04 | 0,07 | 9,44 | 1,44 | 0,06 | 0,02 | 0,56 | 0,12 | 0,32 | bdl | 0,22 | 0,06 | 98,84 |
| **RC4t** | **MIXED ALKALI** | 7,89 | 0,72 | 2,43 | 73,66 | 0,15 | 0,03 | 0,16 | 7,73 | 1,29 | 0,12 | 0,01 | 0,84 | 0,01 | 4,18 | 0,35 | 0,05 | 0,03 | 99,62 |
| **RC8b** | **MIXED ALKALI** | 5,81 | 1,10 | 3,18 | 74,70 | 0,38 | 0,04 | 0,10 | 8,84 | 2,74 | 0,13 | 0,02 | 1,12 | 0,10 | 1,98 | 0,01 | 0,18 | 0,03 | 100,45 |
| **RC11b** | **MIXED ALKALI** | 7,49 | 0,62 | 1,39 | 78,25 | 0,27 | 0,03 | 0,04 | 9,11 | 1,59 | 0,06 | 0,01 | 0,55 | 0,12 | 0,52 | 0,01 | 0,28 | 0,09 | 100,42 |
| **RC12b** | **MIXED ALKALI** | 6,74 | 0,57 | 1,36 | 77,41 | 0,16 | 0,02 | 0,07 | 9,58 | 1,50 | 0,06 | 0,01 | 0,53 | 0,12 | 0,31 | 0,01 | 0,26 | 0,02 | 98,73 |
| **RC13b** | **MIXED ALKALI** | 6,87 | 0,57 | 1,40 | 77,11 | 0,19 | 0,02 | 0,07 | 9,85 | 1,48 | 0,05 | 0,01 | 0,55 | 0,11 | 0,33 | 0,01 | 0,27 | 0,04 | 98,94 |

| Sample | Chemical type | $Na_2O$ | MgO | $Al_2O_3$ | $SiO_2$ | $P_2O_5$ | $SO_3$ | Cl | $K_2O$ | CaO | $TiO_2$ | MnO | FeO | CoO | $Cu_2O$ | $SnO_2$ | $Sb_2O_3$ | PbO | Totals |
|---|---|---|---|---|---|---|---|---|---|---|---|---|---|---|---|---|---|---|---|
| **RC14t** | **MIXED ALKALI** | 5,86 | 0,85 | 2,07 | 74,32 | 0,32 | 0,04 | 0,07 | 9,17 | 2,10 | 0,08 | 0,02 | 0,66 | 0,01 | 4,88 | 0,19 | 0,08 | 0,01 | 100,73 |
| **RC15t** | **MIXED ALKALI** | 5,66 | 0,76 | 1,90 | 74,45 | 0,24 | 0,02 | 0,09 | 9,01 | 1,79 | 0,08 | bdl | 0,61 | 0,02 | 5,05 | 0,24 | 0,07 | 0,03 | 100,02 |
| **RC15w** | **MIXED ALKALI** | 7,11 | 0,74 | 2,61 | 75,49 | 0,28 | 0,06 | 0,08 | 8,93 | 2,07 | 0,09 | 0,02 | 0,61 | bdl | 2,08 | 0,05 | 0,06 | 0,03 | 100,32 |
| **RC16l** | **MIXED ALKALI** | 6,97 | 0,60 | 1,63 | 74,05 | 0,22 | 0,03 | 0,05 | 9,76 | 1,80 | 0,05 | 0,01 | 0,47 | bdl | 3,18 | 0,02 | 0,08 | 0,02 | 98,95 |
| **RC17t** | **MIXED ALKALI** | 8,22 | 0,62 | 1,88 | 73,58 | 0,28 | 0,07 | 0,09 | 8,53 | 2,07 | 0,06 | 0,01 | 0,52 | bdl | 3,96 | 0,13 | 0,07 | 0,02 | 100,13 |
| **RC18t** | **MIXED ALKALI** | 5,74 | 0,91 | 2,39 | 74,07 | 0,30 | 0,05 | 0,11 | 9,17 | 2,13 | 0,10 | 0,02 | 0,74 | 0,01 | 4,83 | 0,19 | 0,07 | 0,04 | 100,87 |
| **RC20g** | **MIXED ALKALI** | 8,12 | 0,62 | 1,52 | 75,37 | 0,19 | 0,03 | 0,16 | 8,68 | 1,50 | 0,08 | 0,01 | 0,90 | 0,10 | 1,07 | 0,02 | 0,28 | 0,03 | 98,68 |
| **TC1l** | **MIXED ALKALI** | 5,94 | 0,84 | 2,30 | 76,91 | 0,18 | 0,04 | 0,08 | 7,91 | 2,12 | 0,10 | 0,02 | 0,76 | 0,01 | 2,67 | 0,09 | 0,08 | 0,03 | 100,09 |
| **TG1l** | **MIXED ALKALI** | 8,26 | 0,88 | 2,11 | 74,37 | 0,19 | 0,03 | 0,12 | 7,62 | 1,73 | 0,08 | 0,02 | 0,68 | 0,01 | 4,42 | 0,04 | 0,05 | 0,03 | 100,63 |
| **RC6g** | **High-K** | 1,01 | 1,29 | 1,61 | 68,60 | 0,72 | 0,05 | 0,00 | 18,20 | 4,02 | 0,07 | 0,01 | 0,53 | 0,01 | 3,77 | 0,16 | 0,04 | 0,01 | 100,09 |
| **RC7g** | **High-K** | 1,03 | 1,39 | 1,80 | 67,83 | 0,80 | 0,05 | 0,01 | 18,59 | 4,31 | 0,09 | 0,01 | 0,58 | 0,01 | 3,95 | 0,20 | 0,04 | 0,03 | 100,72 |
| **RC14w** | **High-K** | 5,12 | 1,70 | 5,63 | 66,25 | 0,92 | 0,09 | 0,08 | 13,44 | 2,43 | 0,27 | 0,03 | 1,85 | 0,01 | 0,06 | 0,02 | 0,12 | bdl | 98,00 |
| **TC3l** | **High-K** | 2,35 | 0,49 | 1,09 | 73,84 | 0,13 | 0,06 | 0,02 | 15,59 | 1,44 | 0,04 | 0,01 | 0,38 | 0,01 | 4,09 | 0,19 | 0,07 | 0,03 | 99,83 |
| **FM7bl** | **BLACK** | 16,32 | 0,34 | 0,99 | 65,48 | 0,32 | 0,16 | 0,46 | 0,92 | 0,93 | 0,16 | 0,01 | 14,63 | bdl | 0,08 | 0,01 | 0,02 | 0,02 | 100,85 |
| **FM8bl** | **BLACK** | 16,45 | 1,23 | 4,35 | 57,79 | 0,10 | 0,84 | 0,98 | 0,83 | 5,06 | 0,18 | 0,13 | 11,50 | bdl | 0,02 | 0,02 | 0,19 | 2,11 | 101,79 |
| **TG3bl** | **BLACK** | 15,71 | 0,67 | 0,57 | 65,37 | 0,14 | 0,26 | 1,41 | 0,14 | 9,09 | 0,10 | 0,03 | 7,27 | 0,02 | bdl | 0,01 | 0,28 | 0,05 | 101,12 |
| **TG11bl** | **BLACK** | 18,25 | 1,52 | 1,30 | 67,50 | 0,23 | 0,21 | 0,51 | 1,43 | 1,34 | 0,30 | 0,01 | 8,68 | bdl | 0,04 | bdl | 0,07 | 0,03 | 101,42 |
| **TG12bl** | **BLACK** | 14,18 | 1,06 | 2,19 | 62,13 | 0,16 | 0,26 | 0,72 | 0,37 | 3,65 | 0,14 | 0,09 | 8,73 | bdl | 0,03 | 0,02 | 0,06 | 7,17 | 100,95 |
| **TG13bl** | **BLACK** | 18,02 | 0,57 | 0,43 | 66,11 | 0,12 | 0,38 | 1,49 | 0,31 | 8,94 | 0,10 | 0,01 | 3,75 | bdl | 0,03 | 0,02 | 0,81 | 0,08 | 101,16 |
| **FM2y** | **NATRON** | 10,56 | 0,51 | 0,90 | 49,19 | 0,04 | 0,28 | 0,69 | 0,21 | 1,57 | 0,05 | 0,02 | 1,88 | 0,01 | 0,10 | 0,02 | 2,93 | 30,37 | 99,33 |
| **FM8y** | **NATRON** | 8,81 | 0,40 | 1,04 | 48,50 | 0,03 | 0,13 | 0,36 | 0,20 | 1,46 | 0,05 | 0,02 | 3,38 | bdl | 0,12 | 0,02 | 4,36 | 30,19 | 99,06 |
| **FM9y** | **NATRON** | 11,04 | 0,44 | 0,95 | 51,31 | 0,01 | 0,35 | 0,24 | 0,14 | 1,24 | 0,07 | 0,02 | 1,56 | 0,01 | 0,11 | 0,02 | 2,60 | 30,82 | 100,94 |
| **TG12w** | **NATRON** | 15,64 | 0,44 | 0,49 | 70,59 | 0,09 | 0,13 | 1,07 | 1,20 | 6,87 | 0,15 | 0,01 | 4,99 | 0,01 | 0,21 | 0,02 | 0,01 | 0,03 | 101,96 |
| **TG13w** | **NATRON** | 17,14 | 0,60 | 0,36 | 64,28 | 0,06 | 0,24 | 1,49 | 0,23 | 9,11 | 0,01 | 0,02 | 0,32 | bdl | 0,02 | 0,04 | 6,95 | 0,07 | 100,95 |
| **FM4inc** | **Classic NATRON** | 18,74 | 0,54 | 0,39 | 67,64 | 0,16 | 0,29 | 1,52 | 0,14 | 9,24 | 0,09 | 0,02 | 0,22 | 0,01 | 0,04 | bdl | bdl | 0,05 | 99,09 |
| **FM5a** | **Classic NATRON** | 17,76 | 0,44 | 0,19 | 74,33 | 0,05 | 0,08 | 0,78 | 0,23 | 6,47 | 0,03 | 0,01 | 0,14 | bdl | 0,11 | 0,01 | bdl | 0,01 | 100,64 |
| **FM10a** | **Classic NATRON** | 18,57 | 0,43 | 0,24 | 74,53 | 0,08 | 0,08 | 0,79 | 0,20 | 6,64 | 0,03 | 0,01 | 0,14 | 0,01 | 0,01 | 0,01 | bdl | 0,04 | 101,80 |
| **FM11a** | **Classic NATRON** | 19,69 | 0,39 | 0,14 | 75,25 | 0,06 | 0,07 | 0,81 | 0,20 | 5,20 | 0,03 | 0,01 | 0,09 | 0,01 | 0,01 | 0,02 | bdl | 0,02 | 101,99 |
| **AM1g** | **Classic NATRON** | 17,38 | 0,63 | 0,33 | 68,51 | 0,06 | 0,25 | 1,19 | 0,06 | 10,53 | 0,13 | 0,01 | 0,28 | bdl | 0,02 | 0,01 | bdl | 0,01 | 99,41 |

Table 2. Major and minor element composition obtained by EMPA on the analysed samples (oxide weight %). bdl= below detection limit.

Table 3

| SAMPLE | Chemical type | Ti | V | Cr | Co | Ni | Cu | Zn | Ga | As | Rb | Sr | Y | Zr | Nb | Sn | Sb | Ba | Hf | Ta | Th | U |
|---|---|---|---|---|---|---|---|---|---|---|---|---|---|---|---|---|---|---|---|---|---|---|
| **GC2a** | **LMLK** | 421 | 8,89 | 13,82 | 1,46 | 3,97 | 2,56 | 9,92 | 3,19 | n.a. | 10,03 | 272,83 | 4,20 | 29,06 | 1,36 | 0,54 | 0,00 | 185 | 0,74 | 0,09 | 0,71 | 0,67 |
| **PM1g** | **PLANT ASH** | 291 | 7,56 | n.r. | 2,70 | 14,67 | 6051 | 102 | 0,71 | 44,48 | 11,27 | 344 | 1,74 | 7,24 | 0,57 | 256 | 26,24 | 54 | 0,19 | 0,03 | 0,38 | 0,16 |
| **V1l** | **PLANT ASH** | 299 | 9,34 | n.r. | 7,84 | 20,41 | 7711 | n.d | 1,44 | 11,86 | 9,73 | 276 | 2,51 | 12,19 | 1,06 | 9,15 | 2,13 | 36 | 0,36 | 0,09 | 0,75 | 0,21 |
| **MT2t** | **PLANT ASH** | 147 | 4,91 | n.r. | 8,52 | 11,99 | 8252 | 31,08 | 0,49 | 7,19 | 5,93 | 450 | 1,54 | 7,04 | 0,52 | 8,45 | n.d | 31 | 0,21 | 0,03 | 0,38 | 0,15 |
| **MON3g** | **PLANT ASH** | 396 | 14,34 | 28,94 | 2,79 | 35,31 | 513 | 19,51 | 1,67 | 4,33 | 9,09 | 428 | 2,68 | 14,68 | 0,99 | 5,10 | 424 | 44 | 0,31 | 0,08 | 0,54 | 0,22 |
| **MON6g** | **PLANT ASH** | 290 | 9,42 | 29,90 | 5,04 | 38,85 | 4501 | 14,51 | 1,23 | 5,34 | 6,13 | 430 | 2,65 | 11,62 | 0,79 | 8,24 | 1,79 | 31 | 0,24 | 0,04 | 0,41 | 0,15 |
| **FM3inc** | **PLANT ASH** | 318 | 10,94 | 14,10 | 1,94 | 10,16 | 14,60 | 33,14 | 2,18 | 4,44 | 5,97 | 236 | 1,62 | 12,18 | 0,95 | 2,03 | 322,08 | 27 | 0,27 | 0,04 | 0,36 | 0,92 |
| **FM6l** | **PLANT ASH** | 309 | 8,59 | 14,45 | 13,83 | 20,33 | 7729 | 67,22 | 1,45 | 4,95 | 5,23 | 342 | 1,98 | 13,87 | 0,92 | 97,52 | 196,00 | 62 | 0,22 | 0,06 | 0,31 | 0,60 |
| **TG5l** | **PLANT ASH** | 284 | 9,10 | 34,70 | 5,43 | 18,12 | 9004 | 25,78 | 1,26 | 11,34 | 12,69 | 299 | 2,22 | 11,57 | 0,85 | 12,99 | 2,05 | 36 | 0,29 | 0,05 | 0,54 | 0,19 |
| **TG7inc** | **PLANT ASH** | 360 | 8,54 | 6,02 | 1,24 | 3,24 | 39,46 | 12,06 | 0,99 | 0,59 | 6,85 | 226 | 1,51 | 15,10 | 0,87 | 1,91 | 0,23 | 34 | 0,38 | 0,05 | 0,34 | 0,23 |
| **TG8l** | **PLANT ASH** | 360 | 9,84 | 2,70 | 14,40 | 16,45 | 5768 | 108,62 | 1,07 | 10,41 | 4,73 | 303 | 1,82 | 15,45 | 0,87 | 455 | 322 | 43 | 0,37 | 0,05 | 0,35 | 0,39 |
| **TG9l** | **PLANT ASH** | 611 | 13,03 | n.r. | 11,64 | 25,79 | 8019 | 61,82 | 1,56 | 3,81 | 5,86 | 425 | 3,25 | 26,86 | 1,45 | 36,69 | 1,81 | 409 | 0,68 | 0,08 | 0,73 | 0,59 |
| **TG10l** | **PLANT ASH** | 341 | 9,89 | 42,45 | 6,46 | 23,13 | 7258 | 36,78 | 1,20 | 17,00 | 10,42 | 442 | 2,42 | 14,40 | 0,91 | 24,49 | 37,51 | 38 | 0,33 | 0,04 | 0,54 | 0,21 |
| **TG14l** | **PLANT ASH** | 377 | 4,63 | n.r. | 2,34 | 3,79 | 5032 | 14,95 | 0,67 | 7,23 | 3,99 | 384 | 1,86 | 21,79 | 0,87 | 257 | 3,29 | 40 | 0,49 | 0,08 | 0,63 | 0,16 |
| **TG17l** | **PLANT ASH** | 365 | 10,57 | 35,72 | 5,43 | 21,83 | 6746 | 34,61 | 1,15 | 11,99 | 9,44 | 478 | 2,52 | 15,44 | 0,90 | 15,20 | 36,94 | 38 | 0,35 | 0,05 | 0,64 | 0,20 |
| **BDT1l** | **MIXED ALKALI** | 454 | 9,57 | n.r. | 13,92 | 28,02 | 20971 | 156 | 2,19 | 27,19 | 117 | 154 | 3,53 | 24,97 | 1,89 | 968 | 17,81 | 72 | 0,57 | 0,15 | 1,42 | 0,28 |
| **MON1b** | **MIXED ALKALI** | 379 | 8,13 | 12,24 | 992 | 1834 | 5729 | 64 | 1,79 | 1233 | 112 | 87,22 | 2,49 | 18,64 | 1,16 | 119 | 1074 | 47 | 0,51 | 0,10 | 1,11 | 0,25 |
| **MON2b** | **MIXED ALKALI** | 538 | 10,95 | 11,62 | 783 | 4940 | 16675 | 1258 | 2,86 | 2432 | 138 | 116 | 3,34 | 34,88 | 2,51 | 11,35 | 3214 | 67 | 0,84 | 0,17 | 1,56 | 0,41 |
| **MON4l** | **MIXED ALKALI** | 429 | 9,41 | 13,81 | 10,26 | 17,28 | 27065 | 90,34 | 2,58 | 15,42 | 139 | 119 | 3,08 | 21,49 | 1,47 | 72,02 | 10,00 | 53 | 0,59 | 0,12 | 1,22 | 0,33 |
| **MON5l** | **MIXED ALKALI** | 359 | 7,64 | 13,12 | 11,29 | 12,24 | 24017 | 67,08 | 1,82 | 15,75 | 123 | 98,59 | 2,64 | 18,06 | 1,18 | 125 | 6,94 | 46 | 0,54 | 0,11 | 1,01 | 0,27 |
| **MON7l** | **MIXED ALKALI** | 493 | 10,33 | 16,20 | 12,35 | 17,64 | 20233 | 66,24 | 2,24 | 18,25 | 154 | 93,39 | 3,04 | 20,27 | 1,38 | 1052 | 11,44 | 44 | 0,51 | 0,09 | 1,17 | 0,28 |
| **RC2b1** | **MIXED ALKALI** | 350 | 7,35 | 8,53 | 893 | 2353 | 2378 | 37,49 | 1,94 | 1396 | 123 | 99,65 | 2,33 | 17,56 | 1,23 | 16,53 | 1440 | 36 | 0,46 | 0,10 | 1,18 | 0,24 |
| **RC2b2** | **MIXED ALKALI** | 341 | 7,53 | 7,70 | 957 | 2489 | 3603 | 36,77 | 1,89 | 1520 | 108 | 95,39 | 2,33 | 16,72 | 1,16 | 15,90 | 1744 | 33 | 0,41 | 0,10 | 1,05 | 0,23 |
| **RC2b3** | **MIXED ALKALI** | 336 | 7,37 | 7,70 | 876 | 2251 | 2276 | 36,69 | 1,98 | 1355 | 114 | 97,07 | 2,41 | 17,19 | 1,18 | 14,34 | 1400 | 33 | 0,42 | 0,10 | 1,11 | 0,24 |
| **RC3b1** | **MIXED ALKALI** | 337 | 7,64 | 8,41 | 915 | 2353 | 2450 | 39,03 | 1,89 | 1427 | 113 | 105 | 2,56 | 17,68 | 1,17 | 16,35 | 1473 | 28 | 0,45 | 0,11 | 1,18 | 0,20 |
| **RC3b2** | **MIXED ALKALI** | 346 | 7,30 | 5,15 | 871 | 2251 | 2271 | 35,69 | 1,83 | 1284 | 112 | 99,84 | 2,51 | 17,88 | 1,16 | 15,89 | 1332 | 41 | 0,51 | 0,11 | 1,16 | 0,20 |
| **RC4t** | **MIXED ALKALI** | 670 | 13,25 | 24,76 | 17,04 | 34,47 | 27848 | 75,06 | 2,80 | 33,10 | 118 | 102 | 4,16 | 25,01 | 1,95 | 2017 | 24,44 | 63 | 0,67 | 0,12 | 1,76 | 0,32 |
| **RC8b** | **MIXED ALKALI** | 716 | 16,23 | n.r. | 807 | 1636 | 13112 | n.d | 3,78 | 1230 | 107 | 153 | 5,41 | 36,26 | 2,26 | 88,09 | 1060 | 89 | 0,99 | 0,22 | 2,13 | 0,40 |
| **RC11b** | **MIXED ALKALI** | 351 | 7,33 | 6,17 | 1046 | 2671 | 4808 | 47,71 | 1,76 | 1701 | 96,99 | 95,14 | 2,33 | 17,28 | 1,08 | 18,63 | 2199 | 41 | 0,42 | 0,10 | 1,02 | 0,18 |
| **RC12b** | **MIXED ALKALI** | 351 | 7,65 | 7,71 | 870 | 2210 | 2279 | 31,89 | 1,87 | 1269 | 116 | 109 | 2,99 | 20,28 | 1,26 | 18,87 | 1340 | 33 | 0,52 | 0,10 | 1,28 | 0,22 |
| **RC13b** | **MIXED ALKALI** | 336 | 7,56 | 6,43 | 881 | 2262 | 2263 | 33,23 | 1,85 | 1342 | 116 | 102 | 2,62 | 17,90 | 1,21 | 14,53 | 1362 | 30 | 0,49 | 0,11 | 1,19 | 0,22 |
| **RC14t** | **MIXED ALKALI** | 420 | 9,70 | 13,81 | 16,35 | 22,62 | 26918 | 61,30 | 2,37 | 21,29 | 95 | 103 | 3,27 | 22,04 | 1,39 | 1010 | n.d | 37 | 0,50 | 0,08 | 1,25 | 0,29 |

| SAMPLE | Chemical type | Ti | V | Cr | Co | Ni | Cu | Zn | Ga | As | Rb | Sr | Y | Zr | Nb | Sn | Sb | Ba | Hf | Ta | Th | U |
|---|---|---|---|---|---|---|---|---|---|---|---|---|---|---|---|---|---|---|---|---|---|---|
| **RC15t** | **MIXED ALKALI** | 429 | 10,17 | 16,02 | 20,90 | 24,48 | 34940 | 49,56 | 2,49 | 33,87 | 105 | 100 | 3,14 | 22,10 | 1,53 | 1595 | 5,64 | 36 | 0,56 | 0,13 | 1,18 | 0,28 |
| **RC16l** | **MIXED ALKALI** | 355 | 6,76 | 13,17 | 9,79 | 11,66 | 17171 | 91,28 | 1,97 | 44,38 | 154 | 107 | 3,01 | 22,48 | 1,88 | 29,33 | 99,23 | 61 | 0,59 | 0,19 | 1,17 | 0,41 |
| **RC17t** | **MIXED ALKALI** | 361 | 8,55 | 10,06 | 14,82 | 22,25 | 27480 | 97,96 | 2,24 | 29,05 | 142 | 139 | 2,95 | 19,85 | 1,40 | 3941 | 10,04 | 47 | 0,52 | 0,11 | 1,20 | 0,27 |
| **RC18t** | **MIXED ALKALI** | 507 | 11,32 | 16,95 | 19,81 | 30,54 | 34664 | 72,81 | 2,79 | 35,96 | 113 | 118 | 3,85 | 27,21 | 1,68 | 1936 | 19,83 | 48 | 0,64 | 0,14 | 1,53 | 0,35 |
| **RC20g** | **MIXED ALKALI** | 394 | 8,89 | 16,37 | 947 | 2103 | 7778 | 207 | 1,88 | 1471 | 98,01 | 78,02 | 2,27 | 16,23 | 1,15 | 82,07 | 2010 | 38 | 0,37 | 0,08 | 1,00 | 0,24 |
| **TG1l** | **MIXED ALKALI** | 446 | 10,34 | 11,83 | 7,62 | 15,03 | 27143 | 66,80 | 2,55 | 18,73 | 99,34 | 89,70 | 3,08 | 19,12 | 2,36 | 175 | 17,81 | 49 | 0,51 | 0,17 | 1,51 | 0,38 |
| **RC6g** | **High-K** | 451 | 8,30 | n.r. | 19,83 | 35,47 | 25599 | 62,89 | 2,59 | 39,80 | 179 | 257 | 3,62 | 37,93 | 3,26 | 1129 | 21,54 | 87 | 0,85 | 0,21 | 1,57 | 0,36 |
| **RC7g** | **High-K** | 481 | 11,15 | n.r. | 1106 | 2457 | 8723 | 208 | 2,64 | 1576 | 116 | 105 | 3,13 | 20,58 | 1,49 | 101,97 | 2185 | 52 | 0,34 | 0,07 | 1,25 | 0,25 |
| **FM7bl** | **BLACK** | 881 | 23,23 | 35,36 | 5,02 | 35,51 | 463 | 26,97 | 4,19 | 12,32 | 15,92 | 148 | 5,24 | 39,15 | 2,54 | 7,43 | 2401 | 189 | 0,99 | 0,15 | 2,64 | 5,18 |
| **FM8bl** | **BLACK** | 701 | 109,01 | 42,39 | 3,55 | 21,64 | 202 | 9253 | 4,51 | 300 | 19,75 | 122 | 7,29 | 44,62 | 2,30 | 19,48 | 1680 | 106 | 1,07 | 0,15 | 1,95 | 4,60 |
| **TG3bl** | **BLACK** | 441 | 10,47 | 11,41 | 15,28 | 17,42 | 9,65 | 4,60 | 1,32 | 1,26 | 0,34 | 241 | 4,94 | 63,54 | 1,33 | 6,09 | 1760 | 19 | 1,38 | 0,07 | 0,54 | 1,14 |
| **TG12bl** | **BLACK** | 712 | 5,75 | 11,80 | 6,84 | 8,14 | 7,94 | 5,57 | 1,24 | 0,59 | 0,73 | 161 | 4,03 | 146,81 | 2,03 | 7,36 | 166 | 24 | 3,30 | 0,15 | 0,68 | 2,05 |
| **TG13bl** | **BLACK** | 510 | 6,99 | 12,47 | 8,27 | 11,08 | 86,49 | 6,24 | 1,17 | 1,31 | 1,39 | 232 | 4,32 | 69,89 | 1,44 | 8,20 | 5403 | 15 | 1,55 | 0,08 | 0,55 | 0,76 |
| **FM4inc** | **Classic NATRON** | 385 | 4,44 | n.r. | 1,28 | 6,88 | 50,78 | 36,39 | 0,78 | 1,42 | 1,17 | 281 | 4,05 | 120,08 | 1,12 | 4,70 | 0,58 | 94 | 2,65 | 0,07 | 0,50 | 0,76 |
| **FM5a** | **Classic NATRON** | 104 | 2,94 | n.r. | 0,97 | 5,21 | 44,44 | 28,46 | 0,31 | 0,69 | 1,97 | 168 | 0,97 | 7,26 | 0,28 | 12,26 | 3,52 | 35 | 0,16 | 0,01 | 0,14 | 0,35 |
| **FM10a** | **Classic NATRON** | 114 | 3,01 | 1,82 | 0,44 | 3,18 | 9,03 | 13,14 | 0,60 | n.d | 1,71 | 174 | 1,12 | 8,04 | 0,31 | 5,67 | 2,31 | 32 | 0,18 | 0,01 | 0,18 | 0,35 |
| **FM11a** | **Classic NATRON** | 78 | 2,34 | 2,73 | 0,48 | 1,79 | 5,68 | 5,65 | 0,24 | 0,10 | 1,93 | 164 | 0,98 | 7,19 | 0,22 | 5,47 | 4,48 | 32 | 0,15 | 0,01 | 0,12 | 0,46 |
| **AM1g** | **Classic NATRON** | 627 | 5,07 | n.r. | 1,24 | 6,97 | 5,09 | 13,62 | 0,81 | 1,15 | 0,56 | 296 | 4,25 | 201,64 | 1,66 | 6,10 | 0,30 | 22 | 4,16 | 0,10 | 0,50 | 0,99 |

Table 3. Trace-element composition obtained by LA-ICPMS on the analysed samples (in ppm). n.r.= not reported. n.d.= not detected.

Table 4

| SAMPLE | Chemical type | La | Ce | Pr | Nd | Sm | Tb | Dy | Ho | Er | Tm | Yb | Lu |
|---|---|---|---|---|---|---|---|---|---|---|---|---|---|
| **GC2a** | **LMLK** | 5,55 | 12,57 | 1,37 | 4,48 | 0,86 | 0,14 | 0,69 | 0,17 | 0,39 | 0,07 | 0,38 | 0,07 |
| **PM1g** | **PLANT ASH** | 2,01 | 3,46 | 0,38 | 1,91 | 0,30 | 0,07 | 0,31 | 0,05 | 0,18 | 0,02 | 0,17 | 0,01 |
| **V1l** | **PLANT ASH** | 2,44 | 4,93 | 0,52 | 2,34 | 0,58 | 0,11 | 0,49 | 0,08 | 0,29 | 0,04 | 0,28 | 0,02 |
| **MT2t** | **PLANT ASH** | 1,51 | 3,21 | 0,34 | 1,50 | 0,45 | 0,07 | 0,31 | 0,04 | 0,16 | 0,02 | 0,15 | 0,01 |
| **MON3g** | **PLANT ASH** | 2,68 | 5,12 | 0,58 | 2,45 | 0,55 | 0,08 | 0,46 | 0,10 | 0,27 | 0,04 | 0,27 | 0,04 |
| **MON6g** | **PLANT ASH** | 2,43 | 4,85 | 0,50 | 2,31 | 0,43 | 0,08 | 0,49 | 0,08 | 0,25 | 0,04 | 0,15 | 0,03 |
| **FM3inc** | **PLANT ASH** | 3,30 | 23,08 | 0,76 | 2,79 | 0,48 | 0,05 | 0,29 | 0,05 | 0,15 | 0,02 | 0,13 | 0,01 |
| **FM6l** | **PLANT ASH** | 2,50 | 13,49 | 0,55 | 2,39 | 0,58 | 0,09 | 0,33 | 0,06 | 0,26 | 0,02 | 0,17 | 0,02 |
| **TG5l** | **PLANT ASH** | 2,26 | 4,50 | 0,49 | 2,17 | 0,46 | 0,11 | 0,40 | 0,07 | 0,23 | 0,03 | 0,19 | 0,03 |
| **TG7inc** | **PLANT ASH** | 2,05 | 4,95 | 0,45 | 1,77 | 0,36 | 0,05 | 0,27 | 0,05 | 0,15 | 0,02 | 0,15 | 0,02 |
| **TG8l** | **PLANT ASH** | 2,04 | 4,91 | 0,45 | 1,80 | 0,42 | 0,06 | 0,34 | 0,07 | 0,18 | 0,02 | 0,17 | 0,02 |
| **TG9l** | **PLANT ASH** | 3,52 | 6,61 | 0,80 | 3,36 | 0,68 | 0,13 | 0,53 | 0,10 | 0,32 | 0,04 | 0,22 | 0,04 |
| **TG10l** | **PLANT ASH** | 2,74 | 5,07 | 0,57 | 2,45 | 0,54 | 0,10 | 0,40 | 0,08 | 0,26 | 0,03 | 0,16 | 0,03 |
| **TG14l** | **PLANT ASH** | 2,45 | 3,95 | 0,50 | 2,20 | 0,39 | 0,05 | 0,34 | 0,06 | 0,17 | 0,02 | 0,20 | 0,02 |
| **TG17l** | **PLANT ASH** | 2,62 | 5,14 | 0,54 | 2,42 | 0,66 | 0,11 | 0,48 | 0,10 | 0,27 | 0,03 | 0,19 | 0,04 |
| **BDT1l** | **MIXED ALKALI** | 4,44 | 7,75 | 0,85 | 3,76 | 0,83 | 0,18 | 0,68 | 0,13 | 0,41 | 0,05 | 0,41 | 0,05 |
| **MON1b** | **MIXED ALKALI** | 3,10 | 6,13 | 0,61 | 2,62 | 0,60 | 0,13 | 0,45 | 0,10 | 0,31 | 0,03 | 0,26 | 0,03 |
| **MON2b** | **MIXED ALKALI** | 4,98 | 9,98 | 1,00 | 4,22 | 1,25 | 0,16 | 0,66 | 0,12 | 0,46 | 0,05 | 0,39 | 0,05 |
| **MON4l** | **MIXED ALKALI** | 3,51 | 7,35 | 0,77 | 3,09 | 0,63 | 0,10 | 0,62 | 0,11 | 0,34 | 0,04 | 0,39 | 0,05 |
| **MON5l** | **MIXED ALKALI** | 2,80 | 6,05 | 0,62 | 2,40 | 0,52 | 0,13 | 0,46 | 0,10 | 0,29 | 0,04 | 0,25 | 0,04 |
| **MON7l** | **MIXED ALKALI** | 3,40 | 7,02 | 0,74 | 2,95 | 0,79 | 0,11 | 0,55 | 0,11 | 0,28 | 0,03 | 0,29 | 0,04 |
| **RC2b1** | **MIXED ALKALI** | 3,39 | 7,25 | 0,67 | 2,70 | 0,60 | 0,08 | 0,50 | 0,08 | 0,25 | 0,03 | 0,25 | 0,04 |
| **RC2b2** | **MIXED ALKALI** | 3,17 | 6,93 | 0,63 | 2,56 | 0,52 | 0,07 | 0,48 | 0,07 | 0,22 | 0,03 | 0,22 | 0,03 |
| **RC2b3** | **MIXED ALKALI** | 3,41 | 7,06 | 0,68 | 2,75 | 0,62 | 0,07 | 0,41 | 0,09 | 0,26 | 0,03 | 0,24 | 0,04 |
| **RC3b1** | **MIXED ALKALI** | 3,42 | 7,32 | 0,78 | 2,80 | 0,60 | 0,08 | 0,40 | 0,08 | 0,27 | 0,04 | 0,24 | 0,03 |
| **RC3b2** | **MIXED ALKALI** | 3,44 | 6,82 | 0,67 | 2,74 | 0,56 | 0,08 | 0,50 | 0,10 | 0,26 | 0,04 | 0,28 | 0,03 |
| **RC4t** | **MIXED ALKALI** | 4,60 | 8,69 | 0,90 | 3,91 | 0,90 | 0,19 | 0,72 | 0,15 | 0,53 | 0,06 | 0,48 | 0,07 |
| **RC8b** | **MIXED ALKALI** | 6,39 | 11,27 | 1,33 | 6,13 | 1,31 | 0,25 | 1,13 | 0,20 | 0,64 | 0,07 | 0,58 | 0,09 |
| **RC11b** | **MIXED ALKALI** | 3,25 | 6,63 | 0,64 | 2,61 | 0,64 | 0,11 | 0,45 | 0,08 | 0,30 | 0,03 | 0,27 | 0,03 |
| **RC12b** | **MIXED ALKALI** | 3,82 | 7,61 | 0,75 | 3,12 | 0,65 | 0,10 | 0,54 | 0,10 | 0,31 | 0,03 | 0,37 | 0,02 |
| **RC13b** | **MIXED ALKALI** | 3,43 | 7,39 | 0,71 | 2,74 | 0,59 | 0,09 | 0,47 | 0,09 | 0,27 | 0,03 | 0,27 | 0,03 |
| **RC14t** | **MIXED ALKALI** | 4,06 | 7,86 | 0,85 | 3,55 | 0,64 | 0,13 | 0,54 | 0,11 | 0,27 | 0,04 | 0,43 | 0,02 |

| SAMPLE | Chemical type | La | Ce | Pr | Nd | Sm | Tb | Dy | Ho | Er | Tm | Yb | Lu |
|---|---|---|---|---|---|---|---|---|---|---|---|---|---|
| **RC15t** | **MIXED ALKALI** | 3,74 | 7,92 | 0,82 | 3,24 | 0,70 | 0,11 | 0,59 | 0,11 | 0,33 | 0,04 | 0,34 | 0,03 |
| **RC16l** | **MIXED ALKALI** | 3,40 | 6,60 | 0,71 | 2,86 | 0,61 | 0,14 | 0,59 | 0,10 | 0,36 | 0,05 | 0,28 | 0,04 |
| **RC17t** | **MIXED ALKALI** | 3,26 | 6,96 | 0,71 | 2,90 | 0,59 | 0,09 | 0,49 | 0,10 | 0,26 | 0,03 | 0,33 | 0,04 |
| **RC18t** | **MIXED ALKALI** | 4,61 | 9,42 | 0,98 | 3,91 | 0,82 | 0,12 | 0,70 | 0,13 | 0,42 | 0,04 | 0,44 | 0,06 |
| **RC20g** | **MIXED ALKALI** | 3,05 | 6,66 | 0,64 | 2,67 | 0,74 | 0,11 | 0,46 | 0,08 | 0,30 | 0,03 | 0,20 | 0,03 |
| **TG1l** | **MIXED ALKALI** | 4,21 | 9,05 | 0,84 | 3,38 | 0,63 | 0,09 | 0,58 | 0,12 | 0,31 | 0,05 | 0,29 | 0,04 |
| **RC6g** | **High-K** | 5,49 | 10,18 | 1,11 | 4,38 | 0,95 | 0,10 | 0,76 | 0,13 | 0,45 | 0,05 | 0,40 | 0,06 |
| **RC7g** | **High-K** | 3,77 | 8,18 | 0,79 | 3,52 | 0,87 | 0,12 | 0,42 | 0,06 | 0,26 | 0,03 | 0,22 | 0,02 |
| **FM7bl** | **BLACK** | 8,84 | 14,26 | 1,56 | 6,18 | 1,20 | 0,16 | 0,92 | 0,18 | 0,52 | 0,07 | 0,51 | 0,07 |
| **FM8bl** | **BLACK** | 9,05 | 14,44 | 1,96 | 8,98 | 1,99 | 0,40 | 1,14 | 0,22 | 0,84 | 0,08 | 0,66 | 0,13 |
| **TG3bl** | **BLACK** | 5,04 | 6,74 | 1,03 | 4,50 | 0,86 | 0,14 | 0,74 | 0,17 | 0,44 | 0,05 | 0,40 | 0,05 |
| **TG12bl** | **BLACK** | 4,57 | 6,36 | 0,89 | 3,73 | 0,76 | 0,09 | 0,58 | 0,12 | 0,38 | 0,05 | 0,37 | 0,05 |
| **TG13bl** | **BLACK** | 4,66 | 6,03 | 0,91 | 4,06 | 0,73 | 0,11 | 0,66 | 0,12 | 0,38 | 0,05 | 0,30 | 0,05 |
| **FM4inc** | **Classic NATRON** | 4,15 | 5,83 | 0,84 | 3,55 | 0,67 | 0,12 | 0,60 | 0,12 | 0,42 | 0,05 | 0,36 | 0,05 |
| **FM5a** | **Classic NATRON** | 0,83 | 1,48 | 0,16 | 0,66 | 0,16 | 0,03 | 0,13 | 0,03 | 0,08 | 0,01 | 0,65 | 0,01 |
| **FM10a** | **Classic NATRON** | 1,02 | 1,68 | 0,20 | 0,79 | 0,17 | 0,02 | 0,16 | 0,03 | 0,09 | 0,01 | 0,08 | 0,01 |
| **FM11a** | **Classic NATRON** | 0,71 | 1,29 | 0,14 | 0,65 | 0,14 | 0,02 | 0,13 | 0,03 | 0,09 | 0,01 | 0,07 | 0,01 |
| **AM1g** | **Classic NATRON** | 4,38 | 5,34 | 0,87 | 3,61 | 0,68 | 0,13 | 0,58 | 0,11 | 0,38 | 0,05 | 0,39 | 0,07 |

Table 4. Rare Earth Element composition obtained by LA-ICPMS on the analysed samples (in ppm).

Table 5

| | EBA | MBA2 | MBA3 | RBA | FBA | EIA1-2 | O/A |
|---|---|---|---|---|---|---|---|
| **Grotta Cardini** | 1 | | | | | | |
| **Pompei-S. Abbondio** | 2 | | | | | | |
| **Vivara** | | 2 | | | | | |
| **Murgia Timone** | | | 2 | | | | |
| **Punta di Zambrone*** | | | | 1 | | | |
| **Broglio di Trebisacce** | | | | | 3 | | |
| **Lipari-P. Monfalcone** | | | | | 2 3 | | |
| **Roca Vecchia** | | | | | 3 | | |
| **Torre Castelluccia** | | | | | 3 | | |
| **Cuma**/*** | | | | | | 4 | |
| **Capua**** | | | | | | 2 5 6 | |
| **Pozzuoli***** | | | | | | 4 | |
| **TorreGalli** | | | | | | 3 2 4 | 5 4 |
| **Francavilla** | | | | | | 2 5 4 | 5 |
| **Sarno**** | | | | | | 2 5 4 6 | 2 5 7 |
| **Amendolara** | | | | | | | 5 |

Table 5. Summary of the glass chemical groups present in the Southern Italian sites here analysed , plus those found by Conte and co-workers in other Southern sites (*Conte et al. 2015, **2016a, ***b), in function of their chronology. 1= LMLK; 2= Plant ash; 3= Mixed alkali+High-K; 4= Natron black; 5= classic natron; 6= Al-Co blue; 7=Hig-Alumina.

Table 6

| | EBA | | MBA2 | MBA3-RBA | | | FBA | | EIA1-2 | | | | | O/A | | | |
|---|---|---|---|---|---|---|---|---|---|---|---|---|---|---|---|---|---|
| **Southern Italy** | 1 | 2 | 2 | 2 | | 1 | 2 | 3 | 2 | 3 | 4 | 5 | 6 | 2 | 4 | 7 | 5 |
| **Northern Italy** | 3 | | 3 | 2 | 8 | 1 | 3 | | 2 | 3 | 4 | 5 | 6 | 5 | | | |

Table 6. Comparison between the protohistoric vitreous materials from Southern and Northern Italy. Northern Italian glass data from: EBA: Angelini et al. 2006; MBA2: Angelini et al. 2005; MBA3-RBA: Santopadre and Verità 2000, Angelini et al. 2005; FBA: Brill 1992; Towle et al. 2001; Angelini et al. 2004; EIA 1-2: Angelini et al. 2011, Arletti et al. 2011a; Polla et al. 2011, Conte et al. 2016b, Towle and Henderson 2004; O/A: Angelini et al. 2011. 1= LMLK; 2= Plant ash; 3= Mixed alkali+High-K; 4= Natron black; 5= classic natron; 6= Al-Co blue; 7=Hig-Alumina; 8= HMBG.